

Photoluminescent nanoplateforms in biomedical applications

Ana María Ibarra-Ruiz, Diana C. Rodríguez Burbano & John A. Capobianco

To cite this article: Ana María Ibarra-Ruiz, Diana C. Rodríguez Burbano & John A. Capobianco (2016) Photoluminescent nanoplateforms in biomedical applications, *Advances in Physics: X*, 1:2, 194-225, DOI: [10.1080/23746149.2016.1165629](https://doi.org/10.1080/23746149.2016.1165629)

To link to this article: <https://doi.org/10.1080/23746149.2016.1165629>



© 2016 The Author(s). Published by Taylor & Francis



Published online: 07 Apr 2016.



Submit your article to this journal [↗](#)



Article views: 4228



View related articles [↗](#)



View Crossmark data [↗](#)



Citing articles: 5 View citing articles [↗](#)

Photoluminescent nanoplatforms in biomedical applications

Ana María Ibarra-Ruiz, Diana C. Rodríguez Burbano and John A. Capobianco

Department of Chemistry and Biochemistry and Centre for Nanoscience Research, Concordia University, Montreal, Canada

ABSTRACT

Photoluminescent nanoparticles have evolved during the last decade to become a key component of the biomedical research. Their versatile surface functionalization and adaptable optical properties are some of the remarkable features allowing their implementation for bioimaging and theranostic purposes. This review presents the recent and relevant literature dealing with the synthesis, surface functionalization, and biomedical applications of the most promising photoluminescent nanoparticles (i.e. Au nanoparticles, QDs, Ln-UCNPs, C-dots, and persistent luminescent nanophosphors), as well as a brief summary of the origin of their photoluminescent properties. We also briefly discuss their physicochemical properties, how biocompatible properties have been achieved as well, and the role that both parameters play in the interaction with biological entities.

ARTICLE HISTORY

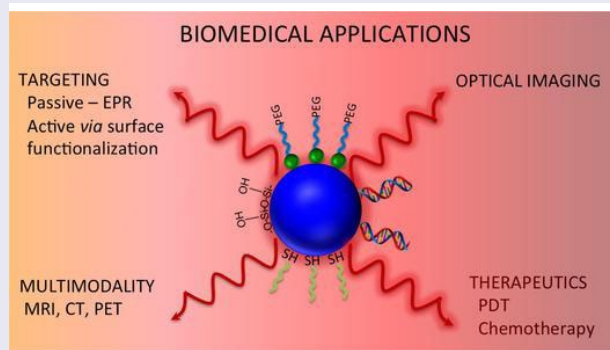
Received 3 December 2015
Accepted 8 March 2016

KEYWORDS

Lanthanide-based nanoparticles; gold nanoparticles; quantum dots and C-dots; upconversion; bioimaging; theranostics

PACS

78.67.-n Optical properties of low-dimensional, mesoscopic, and nanoscale materials and structures; 81.07.-b nanoscale materials and structures: fabrication and characterization; 87.85.Qr nanotechnologies-design; 87.85.Rs nanotechnologies-applications



1. Introduction

Since the moment Richard Feynman sowed the idea to manipulate matter at the atomic scale, nanomaterials emerged as a novel research area that combines the

CONTACT John A. Capobianco  John.Capobianco@concordia.ca

© 2016 The Author(s). Published by Taylor & Francis.

This is an Open Access article distributed under the terms of the Creative Commons Attribution License (<http://creativecommons.org/licenses/by/4.0/>), which permits unrestricted use, distribution, and reproduction in any medium, provided the original work is properly cited.

fundamentals of all natural sciences [1]. Since that time, nanoparticles have been exploited for a wide variety of applications, especially in the biomedical field, where they offer a myriad of exciting possibilities. Nanoparticles are characterized by large surface-to-volume ratios, favoring the loading of therapeutic agents, while their targeting features allow their accumulation in tumor or inflamed tissues. As a result, nanoparticles have the potential to revolutionize the therapeutic strategies currently employed for numerous diseases. Among nanomaterials, photoluminescent nanoparticles can combine the therapeutic effect with bioimaging capabilities. Their remarkable optical properties provide them with the potential in optical imaging (OI), as well as triggering photochemical reactions in biological environments. Accordingly, research has been carried out worldwide leading to the fabrication of superior and biocompatible photoluminescent nanoparticles with controlled size and morphology, particularly semiconductor quantum dots (QDs), lanthanide-based upconverting nanoparticles (Ln-UCNPs), and gold nanoparticles. Such control has allowed their implementation as *in vivo* and *in vitro* OI contrast agents, with excellent detection limit and resolution [2]. Photoluminescent nanoparticles also have been used as building blocks for the fabrication of highly efficient multimodal imaging probes [3, 4]. Consequently, multifunctional nanoplatforms based on this kind of nanostructures are currently in the spotlight with the aim for the development of theranostic agents [5–7].

In this review article, we present the physical fundamentals behind the interesting and unique optical properties of well-known photoluminescent nanoparticles (QDs, gold nanoparticles, and Ln-UCNPs) as well as of the new promising emergent materials (carbon dots [C-dots] and persistent luminescent nanophosphors). We will also discuss the physicochemical properties of these nanoparticles since they are key components to establishing their success in biomedical applications. We discuss how these properties can affect the interaction with biological species and the different surface modification strategies to render them water dispersible and biocompatible. We provide an overview of the most relevant research carried out in the last three years on the development of OI and multimodal imaging and theranostic probes for chemotherapy and photodynamic therapy (PDT) based on the photoluminescent nanoparticles mentioned above. Finally, we show the most relevant findings in terms of the toxicity of nanoparticles.

2. Photoluminescent nanoparticles

2.1. Gold nanoparticles

The outstanding optical properties of gold nanoparticles have propelled them to be considered as a strong alternative to other nanomaterials for the development of biomedical applications. Au is considered a ‘plasma’ metal since it has free and highly mobile electrons with an equal number of fixed positive charges. Au nanoparticles can emit light through the radiative recombination of the exciton

formed by the electrons in the *s-p* conduction band below the Fermi level and the holes in the *d*-bands generated by optical excitation [8]. Upon irradiating the surface of the plasma metal with electromagnetic waves, a collective quantized coherent oscillation of the free electron arises that is in resonance with the frequency of the incident photons. This phenomenon is known as surface plasmon resonance (SPR) [9]. SPR can generate localized and intense optical fields with strong absorption of the incident light. The intensity and wavelength of the SPR band obtained are dependent on the distribution of the electron charge density at the nanoparticle surface, its morphology, size, and the physicochemical properties of the surrounding medium [10]. Two processes contribute to the energy loss of the electromagnetic waves upon interaction with the surface of the metal: (i) light absorption and/or (ii) light scattering. During the light absorption process, the photon energy is dissipated as heat, while in light scattering, the photon energy generates electron oscillations emitting photons as scattered light at the same frequency as the incident light or with a shifted frequency. The contribution of these processes depends on the size and morphology of the nanoparticle [11].

Gold nanoparticles are emerging as promising agents for bioimaging, cancer therapy, and are being investigated as drug carriers and photothermal agents. Common methods for the synthesis of gold nanoparticle include citrate reduction of Au [III] derivatives such as aurochloric acid (HAuCl_4) in water to Au (0) and the Brust-Schiffrin method, which uses two-phase synthesis and stabilization by thiols [12, 13].

For bioimaging applications, the high scattering efficiency of the larger nanoparticles is preferred. On the other hand, smaller nanoparticles are ideal for photothermal therapy due to their capacity of absorbing light and efficiently converting it into heat [14]. A compromise between scattering and absorption processes may be found in Au nanoparticles with distinctive morphologies such as nanorods, nanocages, and nanoshells. Oldenburg et al. developed a synthetic method to obtain Au nanoshells [15]. This core/shell nanostructure is composed of a silica core and a thin gold shell, formed by aging Au clusters found on the surface of the silica core. The SPR band of the nanoshells is composed of the electron oscillations on the inner and outer part of the Au shell. Consequently, the position of the SPR band can be tuned by controlling the shell thickness. Au nanocages were developed by Sun et al. [16]. They were fabricated by a galvanic replacement reaction between silver nanocubes and auric acid. Au nanorods are obtained using the seed-mediated growth method. The growth of the rods is controlled by a surfactant and Ag^+ ions that favor the stabilization of the 1 1 0 plane to a greater extent than the 1 0 0 plane, leading to the faster one-dimensional growth along the [1 0 0] direction [17].

2.2. Quantum dots

Semiconductor QDs are fluorescent inorganic nanocrystals with unique size-dependent optical properties. Their outstanding optical properties include high

quantum yields, broad absorption spectra, large Stokes shifts, tunable narrow emission bands, and high photostability. Typically, QDs are composed from the elements of the groups IV–VI, III–V, and II–VI. Recently, transition metal chalcogenide nanocrystals and ternary alloyed QDs have also been reported [18, 19]. The photophysical properties of the QDs stem from the fact that their physical dimensions (typically 2–10 nm) are smaller than the exciton Bohr radius [20] (the distance between an electron in the conduction band and the hole it leaves behind in the valence band). As size of the QD changes, so does the band gap energy; thus, the optical properties are directly related to the size of the QD. This is known as the quantum confinement effect. The spatial confinement of the exciton increases the energy band gap between the valence band and the conduction band, producing their splitting to discrete energy levels (Figure 1) [21, 22]. The radiative emission arising from the discrete energy levels translates into narrow and symmetric emission bands, product of the radiative electron–hole pair recombination [23]. QDs photoluminescence is also characterized by intermittent on–off states (photoblinking) generally associated with non-radiative deactivations caused by trapping and detrapping events at the nanocrystals surface. Partial suppression of this phenomenon is achieved by isolating the surface using a thin shell of a larger energy band gap material [24]. Recently, Dong et al. demonstrated the fabrication of nonblinking alloyed CdTeS QDs using alkyl thiols as coordinating ligands [25].

A number of synthetic strategies have been developed in order to control the nucleation and growth process such that high-quality QDs are produced. A pioneering approach developed in 1993 by Murray et al. was based on the pyrolysis of organometallic precursors [26]. High-quality QDs were synthesized via the injection of the precursors into a solution with a coordinating ligand to control the growth process. Nevertheless, the organometallic compounds used are commonly toxic and unstable; making them not suitable for large-scale synthesis. Peng et al. described an alternative method using CdO complexed to an alkylphosphonic acid to replace the organometallic precursors, providing a major step toward a green chemistry synthetic strategy [27]. Other parameters have been optimized to develop synthetic routes for the fabrication of high-quality QDs, including the effect of the coordinating ligand [28], solvent [29], and temperature of reaction [30]. However, special attention has been oriented to the development of procedures that produce water-dispersible QDs using hydrophilic molecules to control the reaction kinetics, such as co-precipitation [31], hydrothermal [32], and microwave synthesis [33].

2.3. Lanthanide-doped upconverting nanomaterials (Ln-UCNPs)

Lanthanide-doped upconverting nanoparticles have emerged as an attractive alternative due to their unique optical features. The electronic configuration of the lanthanides ranges from [Xe] $6s^25d^1$ for lanthanum (La) to [Xe] $6s^24f^{14}5d^1$ for lutetium (Lu). The common oxidation state for the lanthanides is 3 + and

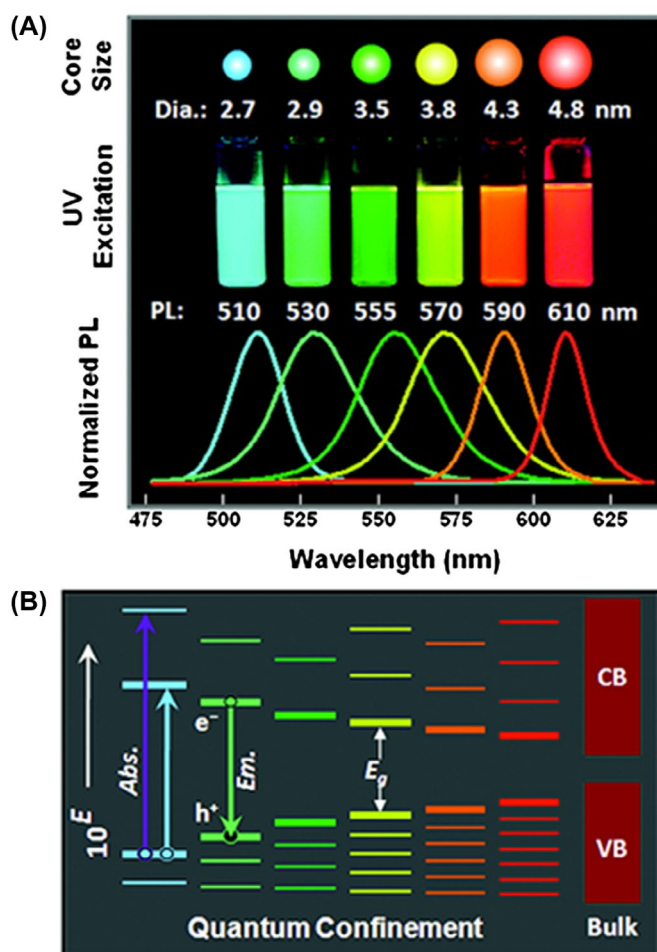


Figure 1. (A) Cartoon, photograph, and PL spectra illustrating progressive color changes of CdSe/ZnS with increasing nanocrystal size. (B) Qualitative changes in QD energy levels with increasing nanocrystal size. Band gap energies, E_g , were estimated from PL spectra. Conduction (CB) and valence (VB) bands of bulk CdSe are shown for comparison. The energy scale is expanded as $10E$ for clarity. Reprinted with permission from [19]. Copyright © 2011, American Chemical Society.

the progression of electron configuration for Ln^{3+} ions is regular from $4f^0$ (La), $4f^1$ (Ce), and $4f^4$ (Lu). The Ln^{3+} ions have xenon-like gas shell of 54 electrons in common and contain N $4f$ electrons with N ranging from zero for La^{3+} to 14 for Lu^{3+} . The electrons in the $4f$ orbitals are shielded by the $5s$ and $5p$ orbitals. Consequently, the optical properties of the lanthanide ions can be attributed to the fact that the $4f$ orbitals are shielded thus minimally affected by the crystal field of the host lattice [34]. Thus, Ln^{3+} ions introduced as dopants in inorganic hosts show narrow absorption and emission bands with long lifetime-excited states. Ln-UCNPs can be excited using near-infrared (NIR) light, and subsequently emit in the ultraviolet (UV), visible (Vis), and NIR regions via the process of upconversion (Figure 2) [35]. This appealing optical property has attracted the

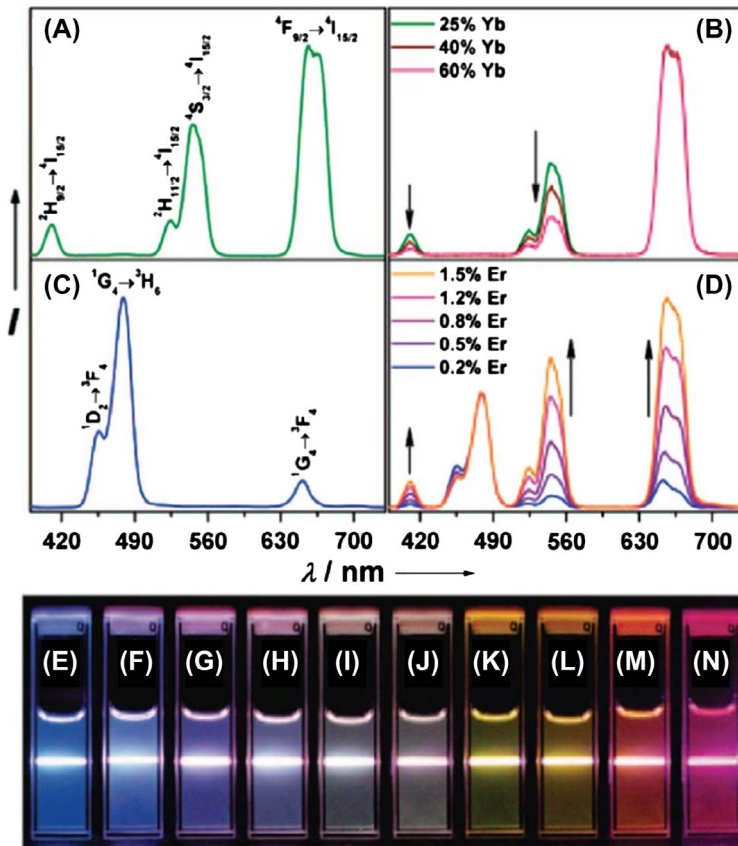


Figure 2. Upconversion emission ($\lambda_{\text{exc}} = 980 \text{ nm}$) for (A) $\text{NaYF}_4:\text{Er}^{3+}/\text{Yb}^{3+}$ (2/18 mol%), (B) $\text{NaYF}_4:\text{Tm}^{3+}/\text{Yb}^{3+}$ (0.2/20 mol%), (C) $\text{NaYF}_4:\text{Er}^{3+}/\text{Yb}^{3+}$ (2/25–60 mol%), and (D) $\text{NaYF}_4:\text{Er}^{3+}/\text{Tm}^{3+}/\text{Yb}^{3+}$ (0.2–1.5/0.2/20 mol%) nanoparticles in ethanol (10 mM). Photos of the emission of colloidal solutions of (E) $\text{NaYF}_4:\text{Tm}^{3+}/\text{Yb}^{3+}$ (0.2/20 mol%), (F–J) $\text{NaYF}_4:\text{Er}^{3+}/\text{Tm}^{3+}/\text{Yb}^{3+}$ (0.2–1.5/0.2/20 mol%), and (K–N) $\text{NaYF}_4:\text{Er}^{3+}/\text{Yb}^{3+}$ (2/25–60 mol%). Camera exposure times of 3.2 s for (E–L) and 10 s for (M) and (N). Reprinted with permission from [34]. Copyright © 2008, American Chemical Society.

attention of researchers in the biomedical field as it circumvents the requirement of UV or Vis light excitations used with other luminescent probes. Moreover, the use of NIR light offers better penetration depth in tissues without imparting damage and avoiding autofluorescence [36]. In addition, Ln-UCNPs do not show photobleaching or photoblinking and there are no size-related effects in their luminescent behavior.

The upconversion luminescence observed in Ln-UCNPs has been explained principally by three major mechanisms, excited state absorption (ESA), energy transfer upconversion (ETU), and photon avalanche (for the purpose of this review, we will only discuss ESA and ETU) [37]. ESA involves the sequential absorption of two or more long-wavelength photons, promoting the ion from the ground to an excited state, followed by the emission of one higher energy photon (shorter wavelength) (Figure 3(A)). ETU occurs via the transfer of energy

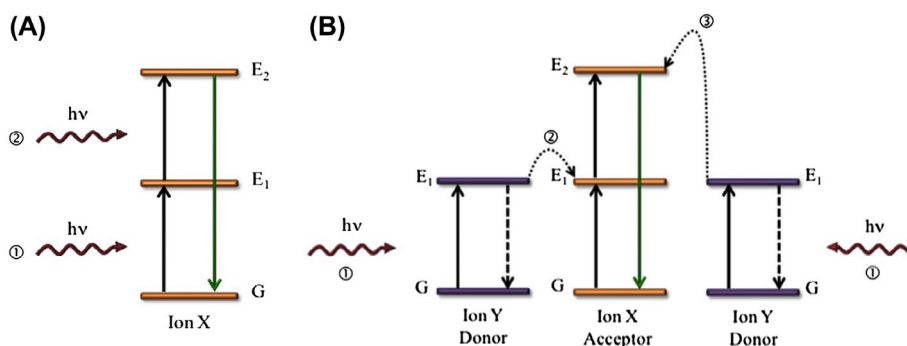


Figure 3. (A) In the ESA mechanism, an incoming pump photon of a wavelength resonant with the $E_1 - G$ energy gap excites ion X from G to E_1 . A second incoming pump photon promotes the ion from E_1 to E_2 , followed by a visible emission and relaxation of the ion to the G state. (B) In the ETU mechanism, an incoming pump photon promotes both donor ions Y (ion with higher absorption cross section) to the intermediate excited state E_1 . A non-radiative energy transfer occurs from the donor ion Y to the acceptor ion X that results in the promotion of the latter to the E_1 . A second energy transfer promotes the acceptor to the excited state E_2 . Finally, the donor ions relax back to their ground state, while the acceptor ion undergoes a radiative decay returning to the ground state. Reprinted with permission from [37]. Copyright © 2015, John Wiley and Sons.

between a donor–acceptor neighboring pair of ions, followed by emission of the acceptor ion (Figure 3(B)). The ETU mechanism is dependent on the overall dopant ion concentration due to the increased proximity of neighboring ion pairs that facilitate the energy transfer process. Therefore, its efficiency is influenced by the choice of donor and acceptor ions, as well as their respective concentrations.

The inorganic crystal host is another important parameter that plays an important role in the efficiency of the upconversion process. An ideal host must possess high chemical stability, low lattice phonon energies that minimize non-radiative process and maximize radiative emissions, and close lattice matches to the dopant ions. These characteristics are exhibited by highly stable fluorides such as NaYF_4 , NaGdF_4 , LiYF_4 , NaLuF_4 with phonon energies $\sim 350 \text{ cm}^{-1}$ [38]. Renero-Lecuna et al. concluded that low-symmetry hosts offer a more highly disorder structures to the emitting ions resulting in a large site distribution. This favors the electronic coupling between the $4f$ energy levels and higher electronic configurations, thus increasing the probabilities of the $f-f$ transitions [39]. Therefore, low-symmetry hosts, such as hexagonal phase of NaGdF_4 or NaYF_4 , exhibit higher upconversion efficiency relative to their cubic counterparts.

It is well established that Ln^{3+} ions, such as Er^{3+} , Tm^{3+} , and Ho^{3+} that have been introduced in the host as emissive centers, possess low-absorption cross sections thus they demonstrate low pump efficiency. In order to enhance the upconversion efficiency, co-doping the host is used. One dopant acts as the activator and the other, usually Yb^{3+} , as the sensitizer. Yb^{3+} has an absorption band at approximately 980 nm with a relatively large absorption cross section that will favor a more efficient ETU mechanism [40].

A conventional synthetic procedure to obtain Ln-UCNPs is the thermal decomposition method [41, 42]. This technique is based on the decomposition of lanthanide trifluoroacetate precursors at high temperatures in a mixture of a high boiling point solvent and a coordinating ligand. While the solvent provides the medium for the reaction, the coordinating ligand controls the growth of the particles. Alternatively, ultra-small Ln-UCNPs (~2–10 nm) with good luminescence efficiency and crystallinity have been synthesized using the ‘high-temperature co-precipitation method.’ In this synthetic strategy, the formation of small amorphous Ln-UCNPs is controlled by a coordinating ligand under room temperature conditions. Subsequently, the temperature is increased to induce the particle growth, producing monodispersed nanocrystals via Ostwald ripening mechanism [43]. These methods produce non-polar colloidally stable Ln-UCNPs. Therefore, the nanoparticles require surface modification to provide dispersibility in aqueous media. An alternative procedure for the fabrication of readily water-dispersible Ln-UCNPs is the hydro(solvo)thermal synthesis. First reported by Heer and co-workers is a solution-based approach that uses supercritical polar solvents to increase the solubility of the lanthanide precursors, favoring the growth rate of the nanoparticles [44]. In addition, surfactants (small molecules and organic polymers) are introduced in the synthesis procedures as nanocrystals growth control agents [45]. This occurs through the formation of a Ln^{3+} -surfactant complex that separates nucleation and growth stages. Thus, the particle size distribution and morphology can be tuned by optimizing the surfactant/ Ln^{3+} ratio [46]. The surfactant also plays the role of capping ligands after the nanoparticles growth stage is terminated, preventing further aggregation [47].

2.4. New emerging photoluminescent nanoparticles

The development of photoluminescent nanoparticles as contrast or theranostic agents promise to make possible the examination of specific biological events and the treatment of diseases with a high degree of selectivity. As a result, novel nanoscale materials providing superior detection limits, multimodal imaging modalities, and improved therapeutic effects are currently under study. Persistent luminescent nanophosphors and C-dots are some examples of the most relevant nanomaterials that have been under investigation as possible alternatives to the traditional luminescent nanoprobes.

2.4.1. Persistent luminescence nanophosphors

The optical properties of the persistent luminescence nanomaterials are based on the recombination of electrons and holes in semiconductor or insulator hosts. When the host is irradiated with a high-energy excitation (X-rays, UV or Vis light), electron holes are generated and trapped in metastable states present in the host. These states, known as trapping sites, may be formed either by the introduction of co-dopants (e.g. lanthanide or transition metal ions), or the presence of

impurities or intrinsic lattice defects. The excitation energy in the trapping sites can be stored for long periods of time and the release can be stimulated either thermally or optically. After the release of electrons, the recombination of electrons and holes produces an emission in the NIR or Vis range of the electromagnetic spectrum [48–53].

The utilization of persistent luminescent nanophosphors as bioimaging contrast agents provides three important advantages: it allows to obtain images without external excitation, eliminating the autofluorescence, and improving the signal-to-noise ratio; emission from persistent luminescence materials are in the range 650–1000 nm which is within the biological optical window, increasing the detection depth; and persistent luminescent nanophosphors may be re-activated after a long period of inactivity using incoherent light sources [52, 54, 55].

Divalent and trivalent lanthanides (Ln, Sm, Eu, Gd, Tb, Dy, Ho, Er, Tm, Yb and Lu) and transition metals (Cr^{3+} and Mn^{2+}) ions have been used as dopant in host such as sulfides, oxysulfides, silicates, germanates, nitrides, stannates, phosphates, aluminates, titanates, metal oxides, and fluorides to obtain red and NIR persistent luminescent materials. The synthetic methods used for the synthesis of persistent luminescent nanophosphors include co-precipitation, sol-gel, and solvothermal techniques followed by high-temperature post-annealing. High-temperature synthesis techniques such as solid-state reaction and combustion synthesis have also been applied [52].

2.4.2. Carbon dots

C-dots recently emerged as excellent and fascinating photoluminescent nanocarbon materials because of their outstanding properties, including water dispersibility, high chemical stability and photostability, low toxicity, and ease of surface modification. C-dots have amorphous or crystalline phase with quasi-spherical shape. They are mainly composed of sp^2 carbon clusters [56] with a high content of oxygen. The incorporation of other heteroatoms has also been explored in order to fine-tune their optical properties [57, 58]. The $\pi \rightarrow \pi^*$ transition of C=C bonds provides them with a strong absorption in the UV region, extending into the Vis range [59]. As well, C-dots exhibit strong photoluminescent emission from the Vis and the NIR [60]. The mechanism of such emission is still a matter of debate and requires further studies. Quantum confinement has been proposed for the size-dependent optical properties demonstrated by C-dots. However, it is believed that C-dots photoluminescence is a surface process rather than related with the sp^2 clusters in the core. Consequently, the radiative recombination of surface-confined electrons and holes might play a major role in the origin of the emission [61]. Therefore, the overall optical behavior of the C-dots is potentially characterized by the competition between the contributions of the quantum confinement effect, emissive traps, and recombination of excitons [62]. In addition, the wavelength of the C-dots emission has been shown to be dependent on the wavelength of excitation. This feature might be attributed to the large heterogeneity in size, chemical

composition, and distribution of emissive trap sites on each C-dot, resulting from the synthetic procedure [60, 63].

The synthetic strategies adopted for the synthesis of C-dots can be classified as top-down or bottom-up approaches. Top-down methods can be carried out breaking off the carbon nanodots from larger carbon structures through chemical, electrochemical, or physical methods. Low-cost precursors, as activated carbon [64], carbon nanotubes [65, 66], soot [67], and graphite [68], have been employed as precursors, enabling potential large-scale production. Bottom-up approaches are based on the pyrolysis or combustion of organic molecular precursors. Heating the precursors above their melting point using simple combustion, plasma, or microwave irradiation leads to the formation of the C-dots, localizing the growth of the nanodots and blocking their agglomeration during the high-temperature treatment [59]. Some of the precursors for this synthetic method include ammonium citrate salts [69], glycerol [70], saccharides [71], and ascorbic acid [72]. These methods constitute an effective and simple alternative for the synthesis of the C-dots and allow the introduction of desirable heteroatoms from the precursors into the nanoparticles.

3. Biomedical applications

3.1. Nanoparticle properties

3.1.1. Size and shape

The success of photoluminescent nanoparticles in bioimaging, drug delivery, and therapeutics is largely dependent on their physicochemical properties. Such properties will primarily determine the interaction with the different bio-entities in the body. Nanoparticles may undergo cellular uptake via pinocytosis. It has been established that there are four possible pathways of pinocytosis of nanoparticles by cells: macropinocytosis, clathrin-mediated endocytosis, caveolae-mediated endocytosis, and clathrin- and caveolae-independent endocytosis [73]. Wang et al. found a general trend demonstrating the dependence of the particles size on cellular uptake [74]. Microparticles possess a slow internalization process carried out through a combination of the different pinocytosis mechanisms, while nanoparticles (10–100 nm) are internalized via a non-clathrin- and non-caveolae-mediated pathway. Nanoparticles with a sphere-like morphology are preferable over other geometries since they circulate predominantly in the center of blood vessel due to distribution of hydrodynamic forces, as well the cellular uptake is more effective due to the lower membrane wrapping time [75].

3.1.2. Surface chemistry

Albeit the size and shape of the nanoparticles that contribute to the cellular uptake, the functional groups at their surface dictate the cell–nanoparticle interaction. Nanoparticles without an appropriate coating or targeting ligands are prone to

nonspecific adsorption of proteins at the surface, leading to particle agglomeration and clearance by the reticular-endothelial system [76]. With a well-designed and optimized surface functionalization, selective and specific recognition of receptors located at the cell membrane can be achieved, as well as enhanced cellular internalization, biocompatibility, and prevention of immune system capture.

The grafting of a silica shell is one most commonly used methods of surface modification. It provides hydrophilic character, stability in aqueous environments, and potential for chemical modification. The two most commonly employed types of silica shells are dense and mesoporous. Dense silica shells are typically synthesized using the ammonia-catalyzed condensation of tetraethyl orthosilicate via the reverse micelle or Stöber method. In the reverse micelle method, the shell is formed in a hydrophilic cavity surrounding the nanoparticle; this cavity is stabilized by surfactant molecules in an organic phase [77]. In the Stöber method, the shell is directly formed at the surface of hydrophilic-functionalized nanoparticles [78]. To graft mesoporous silica shells, hydrophobic nanoparticles are dispersed in the presence of surfactant molecules displacing the hydrophobic ligands and acting as the template for the formation of the porous structure. A novel silica-based nanostructure has been synthesized, which are hollow mesoporous silica shells that offer even higher surface-to-volume ratio and a large pore volume. They are formed after the grafting of two layers of dense silica shells that undergo a surface-protected hot water etching process that breaks the internal Si–O–Si bonds of the first SiO₂ shell and generates mesopores in the second shell [79].

Another preferred surface modification method involves the coating of the surface of nanoparticles using polymers. Polyethylene glycol (PEG) is one of the common polymers used since it has been shown to have a low degree of immunogenicity and antigenicity [54]. In addition, PEGylated nanoparticles are less prone to be uptaken by the reticuloendothelial system, showing longer circulation time in the blood stream thus providing higher accumulation in tumors [80, 81].

A novel alternative, inspired by the cell membrane, is the use of phospholipids as building blocks for the creation of nanostructures, such as liposomes and micelles, to coat photoluminescent nanoparticles. Phospholipid-based coating provides stable dispersion of the nanoparticles in aqueous solution, improved circulation in the blood stream, conjugation to targeting agents, and intrinsic anti-adhesion properties that prevent non-specific interactions at the nanoparticle surface [82].

3.1.3. Targeting

At the nanoscale, particles exhibit the enhanced permeability and retention (EPR) effect, providing them with passive targeting characteristics since they have the tendency to accumulate in tumor or inflamed tissues. However, for biomedical applications, relying only on passive targeting may result in insufficient drug concentration delivered to the diseased tissue due to the presence of several biological barriers, such as the clearance by the reticular-endothelial system [83].

To reinforce the passive targeting, nanoparticles may be conjugated with active targeting agents specific to an overexpressed receptor of the non-healthy cell. Consequently, the nanoparticles may be directed to a specific location, increasing the diagnostic or therapeutic efficacy while reducing side effects. Folate is one of the most commonly used targeting ligands. It has been conjugated to the surface of photoluminescent nanoparticles to carry out the active targeting of tumor cells overexpressing folate receptors, such as ovarian carcinomas, choriocarcinomas, meningiomas, uterine sarcomas, osteosarcomas, and non-Hodgkin's lymphomas [84]. Transferrin, a receptor–ligand pair, has also been investigated for active targeting of tumor cells. Transferrin is a membrane glycoprotein recognized by the transferrin receptor that assists in the cellular uptake of iron via endocytosis and exhibits 10-fold overexpression on cancer cells [85]. Short oligonucleotides of RNA or DNA, also known as aptamers, have also been reported as targeting agents. Aptamers lack immunogenicity and can readily penetrate targeted tumor cells [86]. Alternatively, conjugating antibodies on the surface of nanoparticles can target antigens on the cell membrane. Interestingly, for therapeutic purposes, Mehren et al. reported that when the antibody–antigen interaction occurs, suppression of protein expression can lead to the destruction of tumor cells [87]. In contrast, specific peptides sequences can be used to disrupt ligand–receptor interaction on cancer cells, limiting cellular proliferation [88]. Biju carried out an extensive and detailed review on the available conjugation methods to functionalize photoluminescent nanoparticles with contrast agents, antibodies, peptides, drugs, and genes to develop nanomaterials for targeted imaging and treatment of cancer [89].

3.2. Photoluminescent nanoparticles as imaging probes

3.2.1. Optical imaging (OI)

Optical imaging is a powerful biomedical tool that has been shown to be useful for early detection, screening, and image-guided therapies of various types of diseases [90]. This technique is based on the contrast given by the interaction of the light with a fluorophore. Thus, photoluminescent nanoparticles that serve as OI probes require excitation wavelengths that lie in biological optical transparency windows (BOTW). In this region, light has deeper penetration depth and reduced scattering at the same time autofluorescence from tissues is minimized [55, 91, 92].

QDs, Au nanoparticles, and Ln-UCNPs have been employed, not only for the selective detection of cells, but also for the elucidation of biological processes, identifying intracellular events. Targeting specific molecules in cells and tissues, both *in vitro* and *in vivo*, has been applied to identify molecular events. Alivisatos and coll. were the first to report the functionalization of biotin to CdSe-CdS semiconductor nanocrystals coated with a silica shell [93]. The ligand–receptor interaction avidin–biotin was used to specifically label F-actin filaments in 3T3 mouse fibroblast cells with the biotinylated nanocrystals. Since then, QDs have

become the most popular nanomaterial employed to investigate cellular structures and functions. Thus, numerous review papers have been published on QDs cellular imaging [21, 94–96]. Au nanoparticles also have been exploited in cellular imaging. Their remarkably large absorption cross section makes them suitable as contrast agents in multiphoton luminescence-based techniques. Two-photon absorption can be induced by the excitation of noble metal nanoparticles with a femtosecond pulsed-laser in resonance with their surface plasmon. Au nanocages [97], Au nanorods [98], Au nanoshells [99], and Au nanostars [100] have been reported as contrast agents for two-photon microscopy. In addition, three-photon luminescence (3PL) has been observed in metallic nanoparticles due to their large absorption capabilities. Tong et al. synthesized Au/Ag nanocages which showed two-photon and three-photon luminescence using 760 nm and 1280 nm excitation, respectively [101]. The three-photon luminescence enabled the *ex vivo* detection of intravenously injected nanocages in mouse liver tissue without significant autofluorescence and avoiding the photothermal toxicity associated with two-photon luminescence.

On the other hand, Ln-UCNPs that may be excited by NIR irradiation without requiring high-intensity pulsed lasers have increased their popularity as cellular luminescent probes. Pioneering work using Ln-UCNPs for cellular imaging was reported by Chatterjee et al. [102]. The authors employed polyethylenimine-coated $\text{NaYF}_4:\text{Yb}/\text{Er}$ conjugated with folic acid for *in vitro* imaging of HT29 adenocarcinoma cells and OVCAR3 ovarian carcinoma cells. Bogdan et al. exploited the use of bifunctionalized $\text{NaGdF}_4:\text{Er}/\text{Yb}$ nanoparticles for the *in vitro* imaging of HeLa cells [103]. The UCNPs were functionalized with heparin and basic fibroblast growth factor (bFGF) molecules. The heparin molecules not only provided water dispersibility, but also their interaction with the growth factor resulted in the required conformation of bFGF to interact with receptors on the cell membrane of epithelial cancer cells, optimizing the targeting capabilities of the luminescent nanoprobe. As a result of the number of the potential bio-medical applications of Ln-UCNPs, multiple review papers have been published in the last two years summarizing their potential utilization as cellular imaging probes [37, 104–106].

More recently, non-traditional photoluminescent nanoparticles have been employed as contrast agents for cellular imaging. C-dots constitute an attractive alternative since they show low toxicity and are environmentally friendly. They also exhibit strong two-photon absorption, allowing their application for both, one-photon and two-photon microscopy. Non-specific and targeted imaging has been shown for C-dots, which have been uptaken by multiple kinds of cells, including bacterial and fungal cells [107], HeLa cells [108], fibroblast cells [109], and stem cells [110]. On the other hand, NIR-emitting persistent luminescence nanoparticles have also been applied in cellular imaging. Their ability to undergo optical excitation before being incubated with the targeted cells provides high improvement to the signal-to-noise ratio. The *in vitro* visualization of glioma

cells [111], RAW cells [112], HeLa cells [113], and prostate cancer cells [114] has been achieved.

The prospective of early cancer diagnosis has been one of the driving forces behind the rapid growth of nanotechnology. Photoluminescent nanoparticles have been evaluated as contrast agents for the *in vivo* detection of tumors [115, 116]. One of the first studies reported on *in vivo* cancer imaging using photoluminescent nanoparticles was published by Gao et al. [117]. The authors encapsulated CdSe-ZnS QDs with an ABC triblock co-polymer and linked these nanocomposites to antibody molecules targeted to cancer-specific cell surface biomarkers to perform *in vivo imaging* studies of human prostate cancer growing in nude mice. Under UV irradiation, the CdSe-ZnS displayed red-orange emission. However, the optical features of these luminescent probes are not ideal for bioimaging since they lead to low tissues penetration, high tissue autofluorescence, light scattering, and photodamage are induced using UV light excitation. Accordingly, the development of OI contrast agents for the *in vivo* detection of cancer is currently mostly focused on nanoparticles absorbing and emitting light within the BOTW [55]. Cheng and coll. reported the synthesis of dendron-coated InP-ZnS QDs conjugated with arginine-glycine-aspartic acid peptide dimers suitable for tumor imaging [118]. The dendron-QDs exhibited NIR emission, high stability, biocompatibility, satisfactory *in vivo* pharmacokinetics, and renal clearance. The targeting capabilities of the dendron-QDs resulted in their effective tumor uptake, allowing for the high-resolution imaging of subcutaneous SKOV3 tumors in athymic nude mice. Li et al. have explored lymphatic drainage monitoring and tumor imaging using QDs with emission in the second biological window (1000–1350 nm) [119]. They reported the use of PEGylated NIR Ag₂S QDs ($\lambda_{\text{ems}} = 1200$ nm) for the *in vivo* real-time visualization of lymphatic vessels and lymphatic nodes, blood pool imaging, and tumor angiogenesis through fluorescence imaging upon 808 nm excitation (Figure 4). Bioimaging in the second biological optical window reduces significantly the scattering caused by the tissues, with negligible tissue autofluorescence and increased light penetration, allowing the noninvasive identification of the circulatory systems, thus playing a major role in the diagnosis and therapy of cancer. The use of NIR QDs for the *in vivo* imaging of cancer cells has been widely reported and two excellent reviews have been published [120, 121].

Alternatively, Ln-UCNPs have been proposed as contrast agents for *in vivo* tumor imaging. Chen et al. compared the *in vivo* imaging sensitivity of multilayer oleic acid-polyacrylic acid-PEG coated NaYF₄:Er/Yb UCNPs with that of commercial water-dispersible semiconductor QDs (QD545 and QD625) for the identification of human carcinoma cell tumors in mice [122]. Their results indicate that under their experimental conditions, *in vivo* detection sensitivity of the Ln-UCNPs is one order of magnitude higher than that found for QDs. Although commercial QDs possess higher quantum yield, the detection sensitivity of traditional downconversion luminescent probes is limited by background autofluorescence (Figure 5). This limitation cannot be solved by increasing the

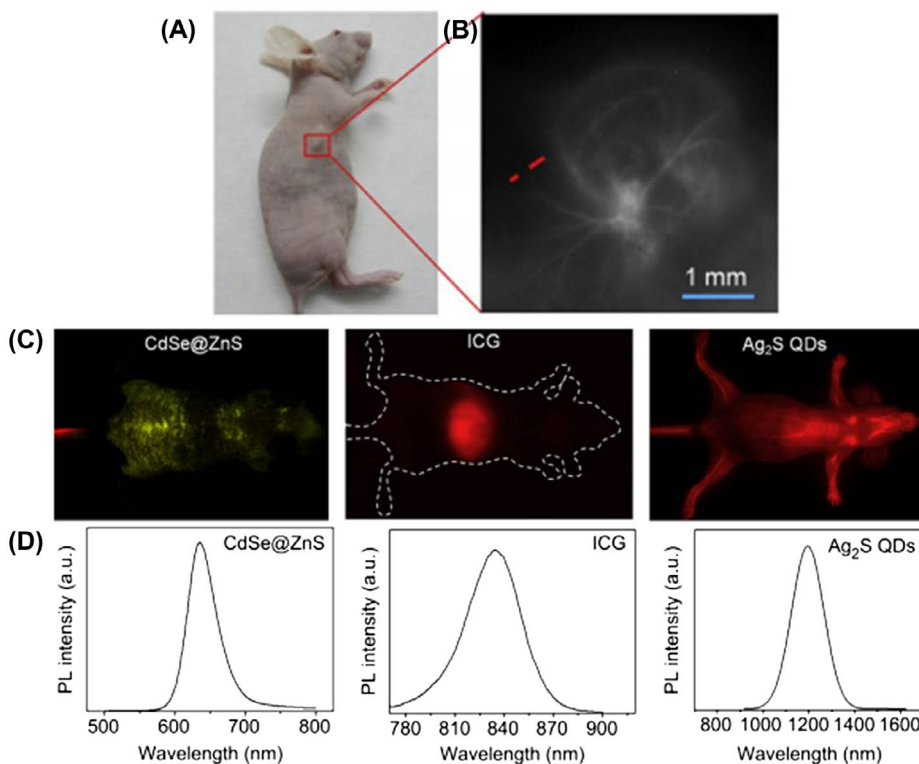


Figure 4. *In vivo* real-time visualization of tumor-induced angiogenesis. NIR-II fluorescence images of the 4T1 mammary tumor-bearing mouse. Fluorescence images were acquired after 30 min post-tail vein injection of PEGylated Ag_2S QDs; (A) Color photo of U87MG tumor-bearing mouse. (B) Amplified fluorescent image of the selected region in (A). (C) *In vivo* fluorescence images of CdSe@ZnS QDs, ICG (NIR-I), and Ag_2S QDs (NIR-II) in nude mice. CdSe@ZnS QDs, ICG, and Ag_2S QDs were injected intravenously into mice and fluorescence images were taken after i.v. injection for 5 min under excitation at 455, 704, and 808 nm, respectively. The green-yellow signal of the mouse injected with CdSe@ZnS QDs indicates the strong autofluorescence of tissues in the visible emission window. The red signal concentrated in the liver of the mouse injected with ICG indicates the short blood circulation half-time. The red signal widely distributed in the whole body of mouse injected with Ag_2S QDs indicates the long blood circulation half-time. (D) The PL spectra of CdSe@ZnS QDs, ICG, and Ag_2S QDs. Reprinted with permission from [118]. Copyright © 2014, Elsevier.

excitation power, or by increasing the time of exposure, nor using better CCD cameras. Thus, given the advantages of using NIR irradiation as excitation source, an increasing number of reports have been published on *in vivo* imaging using Ln-UCNPs [123, 124].

Persistent luminescence nanophosphors were investigated for *in vivo* imaging of tumors for the first time by Scherman and coll [125]. The authors developed PEG-coated $\text{MgSiO}_3:\text{Eu}^{2+}, \text{Dy}^{3+}, \text{Mn}^{2+}$ nanoparticles for the detection of carcinoma cells tumors in mice. The nanophosphors displayed long-lasting afterglow for about 24 h after the UV irradiation was turned off in the red and the NIR attributed to emission from the Mn^{2+} ion. The persistent luminescent nanoparticles were

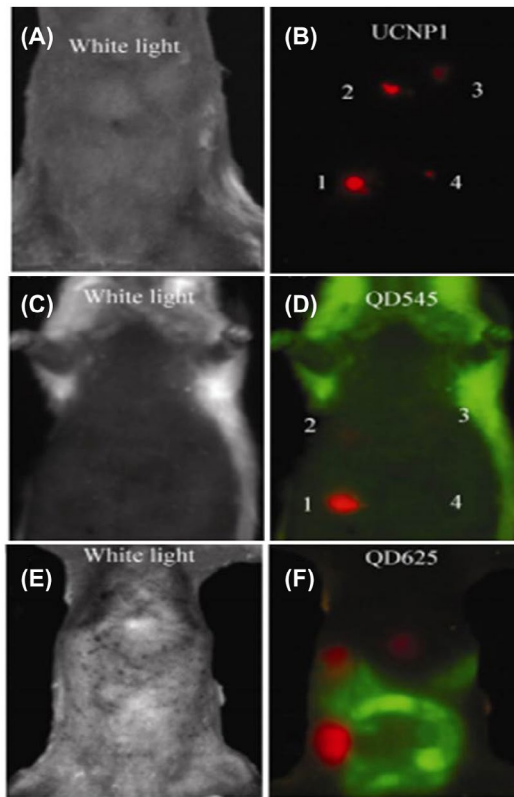


Figure 5. Comparison of imaging sensitivities between UCNP and QDs: (A) white light image of a mouse subcutaneously injected with various concentrations of $\text{NaYF}_4:\text{Er}/\text{Yb}$ UCNP. (B) *in vivo* UCL image of the injected mouse. (C) and (E) white light images of mice subcutaneously injected with QDs; spectrally resolved fluorescence images of QD545 injected mouse (D) and QD 625 injected mouse (F) 625 injected mouse (red and green colors represent QD fluorescence and autofluorescence, respectively). Reprinted with permission from [121]. Copyright © 2010, Tsinghua University Press and Springer-Verlag Berlin Heidelberg.

charged *prior* injection avoiding the tissue autofluorescence and allowing the effective detection of the tumor. Maldiney et al. developed $\text{ZnGa}_2\text{O}_4:\text{Cr}^{3+}$ nanoparticles whose persistent luminescence can be activated not only *ex vivo* before their injection (15 h persistent luminescence emission), but also *in vivo* using photostimulation with low-energy photons (80-min photostimulated emission) [112]. The authors demonstrate the cellular uptake of the nanoparticles via endocytosis through *in vitro* experiments as well, the tracking of labeled cells *in vivo*.

3.2.2. Multimodal imaging

In order to develop imaging procedures providing more accurate detection and clinical diagnosis, contrast agents suitable for OI and with two or more different imaging modalities have been recently studied. Each imaging technique offers complementary information and their synergic integration allows the collection

of more precise information. OI provides high sensitivity but it is limited by low tissue penetration, decreasing its spatial resolution. Therefore, its combination with magnetic resonance imaging (MRI), computed tomography (CT), or positron emission tomography (PET) results in the optimization of space, time, sensitivity, selectivity, and dose properties for efficient *in vitro* and *in vivo* imaging [126].

Dual-mode probes combining light-emitting QDs or Ln-UCNPs with MRI contrast agents have been developed using multiple approaches, including core-shell nanostructures [127], chelate conjugation [128, 129], and Gd^{3+} or Mn^{2+} co-doping [130, 131]. Hu et al. developed a dual-modality nanoprobe based on Ag_2S QDs, which emits in the second biological window and conjugated with the Gd-DOTA MRI contrast agent [132]. This bimodal probe integrates the deep tissue penetration of MRI and takes advantage of the QDs, which have a high signal-to-noise ratio to perform the OI. The authors evaluated the potential of the Gd-DOTA Ag_2S contrast agents for the imaging of U87MG brain tumors in mice in order to guide its surgical resection. According to their results, Gd-DOTA Ag_2S successfully delineated the tumor allowing the precise resection of the tumor. Gd^{3+} -based host Ln-UCNPs such as $NaGdF_4:Ln^{3+}$ have been used as MRI bimodal imaging since these nanoparticles offer a significantly higher number of surface Gd^{3+} ions exposed to water molecules, increasing their r_1 value compared with co-doped nanostructures (e.g. $NaYF_4:Gd^{3+}$). This was shown by Capobianco and coll [133]. The authors recently developed an Ln-UCNP-Gd-chelate bimodal probe by covalent conjugation of Gd-DOTA molecules to citrate-capped $NaGdF_4$ Ln-UCNPs. The presence of the multiple paramagnetic centers in the probe reduced the tumbling rate, improving its relaxivity. The authors reported r_1 values for the nanoconstruct of $25\text{ mM}^{-1}\text{ s}^{-1}$ per Gd^{3+} ion at 60 MHz and 310 K, seven times larger than that of the Gd-DO3A-ethylamine precursor.

PET is a nuclear medicine imaging modality clinically used to produce *in vivo* 3D images. Combining PET with photoluminescent nanoparticles provides an opportunity to obtain more anatomical and physiological details by improving the spatial resolution. Typically, radioactive isotopes conjugated to photoluminescent nanoparticles are ^{18}F [134, 135], ^{53}Sm [136], ^{11}C [137], ^{64}Cu [54, 138, 139], and ^{109}Cd [140]. In addition to their likely use for PET and OI, radiolabeled luminescent nanoparticles also have been explored for their potential in Cerenkov luminescence (CL). Guo et al. synthesized intrinsically radioactive $[^{64}Cu]CuInS/ZnS$ QDs with excellent radiochemical stability [138]. The QDs exhibited self-illuminating behavior without external source of excitation by effect of Cerenkov resonance energy transfer. The radiolabeled QDs were effectively applied as PET/CL contrast agent for the detection of glioblastoma tumor xenografted mouse *in vivo*.

X-ray CT imaging is one of the oldest modalities used for clinical diagnosis. In this technique, CT scanners from different angles detect X-ray radiation and this information is processed to construct 3D images. The X-ray contrast is generated by the difference of attenuation between materials. Typically, X-ray contrast agents

are based on iodinated molecules, because of the high X-ray absorption coefficients, which they manifest. However, iodinated molecules display rapid renal clearance, decreasing the imaging times; as well, they show high kidney toxicity. Alternatively, inorganic nanoparticles, such as gold nanoparticles, iodinated QDs and Ln-UCNPs, have also been explored as X-ray CT contrast agents because of their high X-ray attenuation [141–144].

Recently, the development of photoluminescent nanoprobe suitable for two or more imaging modalities has emerged as a new challenge for the scientific community. These nanomaterials promise to improve the imaging capability providing higher spatial resolution, soft tissue contrast, and higher sensitivity. OI/MRI/CT imaging probes based on photoluminescent nanoparticles have been recently synthesized. Such tri-modal contrast agents combine the high sensitivity of the optical detection with the resolution, 3D visualization, and the excellent tissue penetration of CT and MRI [145–150]. In addition, PET contrast has been introduced into tri-modal luminescent probes [151, 152]. Recently, Rieffel et al. developed a novel multimodal hyper-integrated nanoprobe by coating ^{64}Cu -labeled $\text{NaYbF}_4:\text{Tm}@ \text{NaYF}_4$ Ln-UCNPs with biocompatible porphyrin-phospholipids (PoP) [153]. OI contrast is provided by the NIR upconversion emission of the Tm^{3+} ions and the fluorescence of PoP. The dense self-packing of the spatially constrained PoP bilayer allows for self-quenching, which produces a photoacoustic signal. ^{64}Cu provides both CL and PET imaging capacity. Finally, the CT contrast is induced by the heavy lanthanides in the host matrix. The PoP-coated Ln-UCNPs were evaluated for *in vitro* and *in vivo* lymphatic nodes hexamodal imaging exhibiting good performance in each imaging modality (Figure 6).

3.3. Theranostic nanoplatfoms

Photoluminescent nanoparticles combined with the proper surface functionalization may offer the required multifunctionality to combine disease diagnosis with therapeutic capabilities. Their targeting abilities allow them to accumulate at the disease tissues, while their potential to carry different drugs makes them ideal to provide a site-specific therapeutic effect. In addition, photoluminescent nanoparticles may display an inherent ability to produce reactive oxygen species (ROS), which are important in PDT. Thus, they not only offer multiple imaging modalities but also have the potential to carry out disease diagnosis and monitoring of the treatment response.

3.3.1. Chemotherapy nanoplatfoms

Chemotherapy is one of the most commonly applied therapies for cancer treatment. This therapy is based on the administration of cytotoxic drugs that inhibit the accelerated cellular growth and proliferation. However, despite the excellent anti-cancer character of some commercially available chemotherapy agents, their effectiveness is still limited. The action of chemotherapeutic agents is usually

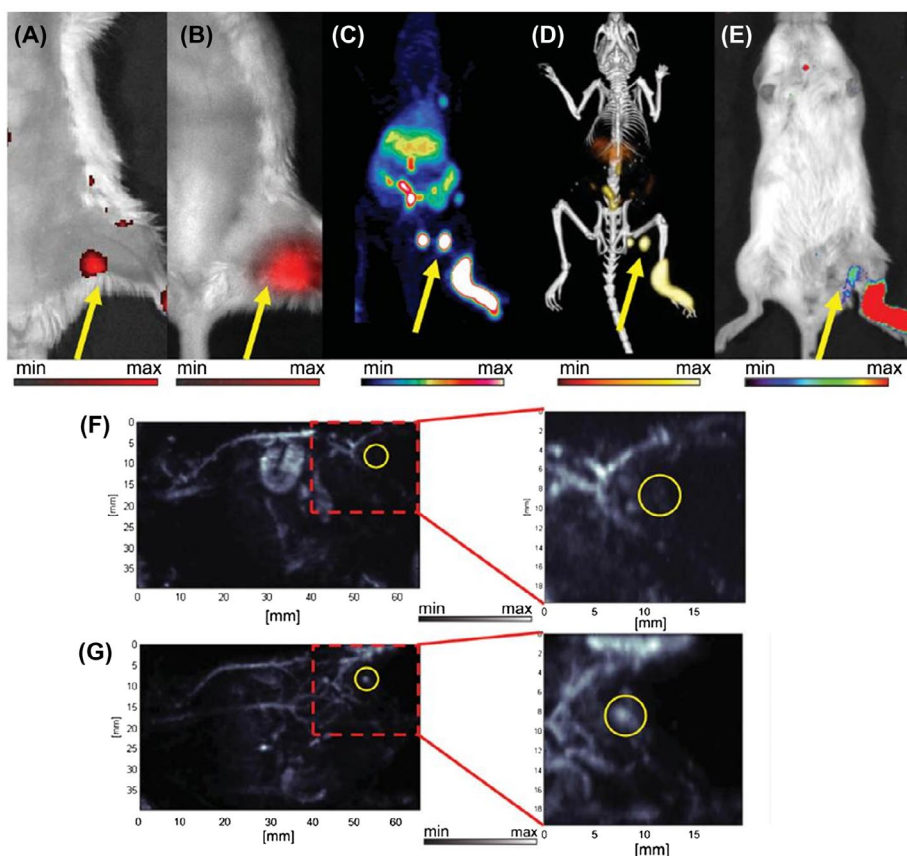


Figure 6. *In vivo* lymphatic imaging using PoP-UCNPs in mice 1 h post-injection. Accumulation of PoP-UCNPs in the first draining lymph node is indicated with yellow arrows. (A) Traditional FL and (B) UC images with the injection site cropped out of frame. (C) Full anatomy PET, (D) merged PET/CT, and (E) CL images. (F) PA images before and (G) after injection show endogenous PA blood signal compared to the contrast enhancement that allowed visualization of the previously undetected lymph node. Reprinted with permission from [152]. Copyright © 2015, John Wiley and Sons.

unspecific and it may induce indiscriminate destruction of cells, generating side effects and restricting the dosage. In addition, the insufficient blood supply of tumor cells reduces the amount of administrated drug molecules reaching the therapeutic site of action, decreasing the efficiency of the treatment [154]. The biomedical field has turned its attention to photoluminescent nanoparticles and their potential as theranostic nanoplatforms. The targeting and surface modification of photoluminescent nanoparticles may constitute the key to overcome the low efficiency faced in the application of chemotherapy. These novels photoluminescent nanoplatforms not only provide imaging contrast, but also carry out light-triggered drug release.

One of the first reports on theranostic nanoplatforms based on photoluminescent nanoparticles was described by Weng et al. [155]. The authors selected

immunoliposomes to encapsulate doxorubicin (DOX) and decorated the surface of the liposomes with HER2 (targeting moiety) and PEGylated QDs as the contrast agents. The authors demonstrated the theranostic effect of the immunoliposome-based nanoplatform on SK-BR-3 and MCF-7/HER2 cells *in vitro* and *in vivo*. After the report of this novel theranostic approach, the use of liposome as carrier for photoluminescent nanoparticles-based theranostic nanoplatforms has encouraged research in this area [155, 156].

PEG coating is another biocompatible alternative that has been widely used to develop theranostic nanoplatforms. This polymer offers a surface that inhibits non-specific binding, as well as an excellent loading capability for therapeutic agents. Polymeric micelles have also been implemented as carriers for theranostic nanoplatforms because of their potential to encapsulated hydrophobic payloads and incorporate multiple functionalities. Wang et al. synthesized a multimodal polymeric micelle bearing a pH-tunable programmable drug release and luminescent QDs for theranostic applications [157]. They employed pH-sensitive PEG-based micelles to control the release of hydrophobic chemotherapy drug molecules under acidic conditions (pH 5) using folic acid as the targeting moiety. These micelles were tested in tumor bearing mice *in vivo*. The authors reported accumulation of the nanocarriers at the tumor site followed by a decrease in tumor size and survival rate of the animals showing the efficacy of the PEG-based micelle as a therapeutic agent.

The grafting of mesoporous silica shells has also been explored for the fabrication of photoluminescent theranostic nanoplatforms [158–161]. Its remarkably high surface area and tunable porous size enable the loading of therapeutic agents at higher levels compared with other carriers. Wang et al. reported a novel upconverting nanotheranostic platform suitable for multimodal imaging and pH-triggered drug delivery [159]. The core of the platform is $\text{NaYF}_4:\text{Yb}/\text{Er}@\text{NaGdF}_4:\text{Yb}$ which is capable of providing three imaging modalities, OI, computer tomography, and MRI. The nanoparticles were coated with a mesoporous silica shell loaded with a chemotherapeutic agent (DOX) onto the porous, while ZnO nanoparticles were employed as ‘gatekeepers’ that efficiently block the mesoporous until their dissolution in the acidic environment in cancer cells induced the DOX release. The evaluation of the performance of the upconverting theranostic nanoplatform incubated with HeLa cells *in vitro* and in tumor-bearing mice *in vivo* indicated a high therapeutic and diagnostic effectiveness for cancer treatment.

3.3.2. Photodynamic therapy

The limitations of the conventional cancer treatments, in terms of specificity and toxicity, have motivated the development of alternative, safe, and effective therapeutic modalities. PDT has emerged as an alternative strategy for tumor ablation. This therapy is based on the localized administration of light-sensitive drug molecules, photosensitizers (PS), followed by irradiation with light of a specific wavelength; this process induces an energy transfer process from the PS to molecular

oxygen triggering the production of cytotoxic ROS, such as singlet oxygen, causing the oxidation of key biomolecules and cellular death [162]. Nonetheless, PDT still has to overcome some challenges to extend their use beyond superficial lesions. First, PS molecules are activated using Vis or UV light, which hinders their use for the treatment of deep-seated tumors. Since it is a localized treatment, reaching the appropriate light dosimetry is still problematic, particularly in solid and bulky tumors; and finally, there is a lack of sufficient selectivity for the tumor tissue, regarding the absence of targeting moieties accompanied by hydrophobic character that limits their bioavailability [163].

Research efforts have been oriented to the use of photoluminescent nanoparticles-based nanoplateforms as the solution to overcome the limitations described earlier. Chang et al. trapped chlorin6 (Ce6) PS molecules in highly fluorescent FA-conjugated PEGylated gold nanoclusters for their application in targeted PDT [164]. The red-emitting Au nanoclusters were employed as OI contrast agents to monitor the accumulation of the theranostic agents at the tumor tissues. The authors report an enhanced efficiency of PDT after *in vitro* and *in vivo* evaluations. Au nanoparticles have also been employed to enhance the absorption of light of the PS by effect of the localized SPR. Chen et al. investigated the enhanced fluorescence and ROS production of porphyrin PS molecules conjugated to silica-coated Au nanorods upon one- and two-photon excitation [165]. They attributed the observed enhancement to a combination of the local electric field amplification and increased radiative decay rates. As well, Förster Resonance Energy Transfer (FRET) has been proposed for the activation of PS to enhance the production of ROS [165, 166]. Martynenko et al. employed ZnSe/ZnS QDs as energy donors for chlorin-Ce6 PS molecules [167]. *In vitro* experiments revealed that the conjugation of the PS molecules with the QDs resulted in a twofold enhancement in the killing of the cancer cell in comparison to the free Ce6 molecules. Ln-UCNPs have also been proposed for the activation of PS molecules. The NIR irradiation used for the excitation of the Ln-UCNPs improves the low tissue penetration exhibited by the red light which is presently used to activate temoporfin [168]. Other PS such as zinc (II) phthalocyanine (ZnPc) [169], aminolevulinic acid (ALA) [170], and chlorin6 (Ce6) [171] have been conjugated to Ln-UCNPs in order to activate the PS via FRET. More recently, TiO₂ has been explored to induce the production of ROS demonstrating low toxicity and stability. Accordingly, multiple groups have reported its activation using Ln-UCNPs [172–176]. Hou et al. developed NaYF₄:Yb³⁺, Tm³⁺@NaGdF₄:Yb³⁺ UCNPs decorated with TiO₂ nanoparticles suitable for PDT *in vivo* [173]. Upon NIR irradiation, the Ln-UCNPs emitted UV light matching the TiO₂ absorption and triggering the ROS production. In addition, the Ln-UCNPs provided OI/MRI/CT multimodal imaging contrast to carry out the monitoring of the therapeutic effect. The implementation of Ln-UCNPs in the development of PDT nanotheranostic agents has been reviewed by Chao Wang et al. [177].

4. Toxicity

As it has been shown in this and other reviews, great effort has been placed in the synthesis and surface modification of photoluminescent nanoparticles, as well as their potential use in different applications such as bioimaging, drug delivery, and therapeutics. However, only in the recent years, toxicity studies have been reported concerning photoluminescent nanomaterials [178].

Nowadays, most of the toxicity studies on nanoparticles are performed using classical toxicology studies, looking at chemical composition and substance dose. Nonetheless, when working with nano-sized materials, it is important to consider several other physicochemical features that might have a toxic effect, including doping, hydrodynamic size, morphology, size heterogeneity, tendency for aggregation, surface functionalization, surface charge, solubility, and biodegradability [179–183]. A significantly lower number of reports are found that study these aspects in detail.

The first and most common step in evaluating nanoparticle toxicity is *in vitro* studies. At this stage, the toxicological effect is assessed on cultured cells. These studies in general consider membrane disruption or permeability, mitochondrial activity, malfunction of enzyme activity, and production of ROS species [184, 185]. The next stage is the introduction of the biocompatible photoluminescent nanoparticles or nanoplateforms to *in vivo* systems, where different physiological considerations need to be taking into account. Intramuscular, subcutaneous, and intravenous injections constitute the most commonly used routes of administration for *in vivo* experiments. In the case of intramuscular and subcutaneous injections, the nanoparticles are deposited and gradually cleared to lymph nodes and the rate of clearance and accumulation in the lymph nodes is dependent on the size and surface chemistry. The larger sizes will exhibit longer retention times in the lymph nodes, while nanoparticles functionalized with ligands with high affinity to phagocytic cells undergo phagocytosis, accumulating in liver and spleen [186, 187]. Intravenously injected nanoparticles are introduced directly into the blood stream, where they could potentially undergo opsonization by the presence of serum proteins. Such process translates in a significant increase in the hydrodynamic size of the nanoparticle, which ultimately has the same fate since they are detected by phagocytic cells [188, 189]. In order to avoid opsonization and phagocytosis, the nanoparticles surface must be modified with an appropriated coating or capping ligand to favor the interaction between the nanoparticles with the membranes in the target cells, which reduces the potential toxicity [180]. Nevertheless, the surface modification may increase the hydrodynamic size of the nanoparticle, which could cause obstruction of blood flow and capillary vessel blockage [189].

Another consequence of the high surface energy exhibited by nano-sized materials is their enhanced potential to interact with proteins and electrolytes in the physiological media, forming agglomerates via electrostatic or hydrophobic

interaction, or chemically bind to form aggregates. These agglomeration results in larger sized materials with decreased surface area and surface charge, minimizing the affinity between nanoparticle and the cell membrane, and possibly increasing toxicological effects [189].

Surface modification strategies, such as silica shell and polymer coatings, are employed to provide biocompatibility and colloidal stability in physiological media to the nanoparticles. However, *in vivo* reports indicated that silica may cause tissue inflammation; this effect may be involved in initiating disorders such as rheumatoid arthritis, sclerosis, lupus, and chronic renal disease [190, 191]. As well, it has been observed that a positively charged surface might cause disruption of the lipid bilayer forming the cell membrane during the nanomaterials cellular uptake [192]. Additionally, the nanoparticles have potential to induce the generation of ROS species, leading to massive cellular death of healthy cells [185].

Review papers summarizing the studies performed on the toxicity of different photoluminescent nanoparticles have been reported, including gold nanoparticles [193–196], QDs [197–201], lanthanide-based nanoparticles [179, 202–204], and C-dots [205]. However, individual toxicity evaluations need to be completed for each developed nanoplatform to completely assure its safety for biomedical applications.

5. Conclusions

Over the past decades, we have witnessed a tremendous growth in the field of nanoscience and nanotechnology. This growth was initially fueled by the fundamental studies of nanomaterials and more recently by the plethora of possible applications. The applications have been driven by the potential integration of nanomaterials in nanomedicine. In this review, we have provided an account of five widely studied nanomaterials, QDs, gold nanoparticles, lanthanide-doped upconverting nanoparticles, persistent nanophosphors, and C-dots with a focus on the synthetic approaches for their preparation, the strategies to achieve surface modifications to accomplish dispersibility in aqueous medium and targeting of specific diseases and imparting multimodality.

QDs have been used as integrated components in assays, bioprobes, and biosensors and as scaffolds for bioconjugation and biorecognition. QDs have emerged as an alternative to fluorescent dyes and over the years their physical and optical properties have been tailored and their permitting greater applications such as their use in imaging methods which includes epifluorescence, confocal, spectral imaging, single particle tracking. In each case, QDs offer many advantages such as brightness, a major requirement needed for sensitive detection, photostability, multiplexing capability, and they serve as nanoscale interface, a requirement in biomolecular engineering. The challenge faced by QDs remains their toxicity; however, their importance will continue to rise as a result of the research being conducted on the use of a core-shell structure.

Due to their chemical inertness, and their ability to tailor the functionality of the surface gold nanoparticles have been used *in vivo* for the past 50 years and have found applications as probes for the diagnosis of cancer cells, delivery vehicles (drugs, genes, proteins), and cancer therapeutics. One of the areas, which needs to be explored, is the molecular interactions of the gold nanoparticles with cells. This fundamental knowledge is required in order to lead to further advances and applications of gold nanoparticles.

Lanthanide-doped upconverting nanoparticles offer significant advantages in nanobiomedicine. These nanoparticles have the unique ability to convert NIR light to higher energy light such as UV, Vis, or NIR (shorter wavelength than the excitation source). The use of NIR excitation allows for deeper tissue penetration, minimized autofluorescence, and reduced photodamage. Thus, upconverting nanoparticles have found widespread application in bioassay, light-triggered photo-release of drugs, activation of PS for PDT, and bioimaging. Fluoride hosts have been the overwhelming choice; however, the full potential of upconverting nanoparticles has not been realized due to the low quantum yields. Thus, it is of paramount importance that fundamental studies be carried out to understand the reasons, which may provide us with insight into the future development of more efficient upconverting nanoparticles.

C-dots resemble graphene oxides both in their chemical structure and physical properties. However, the distinction between them comes from their size since C-dots refer to carbonaceous materials with size below 10 nm. Over the past decade, interest in C-dots has been heightened due to their fluorescent properties. This has propelled chemists, physicists, and material scientists toward research to gain an understanding of the physicochemical properties with the principle goal to unravel the origin of their intrinsic fluorescence, to develop new synthetic strategies, and their biomedical applications, for example, imaging and therapy. However, the community faces a variety of challenges which are not unlike those faced by other photoluminescent nanomaterials; excretion pathway, time required for clearance from the body, pharmacokinetics, and toxicology, quantum yields, surface functionalization and a full understanding of the origin of the intrinsic fluorescence.

Persistent luminescent materials for bioimaging applications have been primarily based on the transition metal ions, Mn^{2+} , and/or Cr^{3+} since they have been found to exhibit persistent luminescence in the NIR region of the spectrum. The most common host materials are in general silicates, phosphates, oxysulfide, and oxides. Unfortunately, these host materials agglomerate and are not water dispersible. Therefore, further investigations are required to develop new host materials which are dispersible in aqueous media yet maintain their persistent luminescence properties. In addition, the community must endeavor to develop multimodal persistent phosphors that may be used both in OI and as magnetic probes. Effective surface functionalization and biocompatibility issues must be addressed. More efforts are required for the development of lanthanide-based

NIR persistent luminescent materials that exhibit long persistent luminescence (hours). This would enhance their potential application in bioimaging.

The unique optical and physicochemical properties of each of the luminescent nanomaterials discussed in this review contribute to making them highly attractive candidates for imaging, drug delivery, targeting, detection, and therapy. Although much progress has been made over the past years, further studies of imaging approaches, drug delivery, and therapeutics are required, which address uptake, release rate, toxicity of both the nanoparticle and the drug. These studies are essential and will provide a fundamental insight into the mechanism of uptake of nanoparticles by cells. At the nanometer scale, the surface is a very important parameter that cannot be ignored, since the majority of atoms lie there. Therefore, an understanding of the surface interactions with biological molecules is required, since this may not only determine the fate of the nanoparticles in the body, but also their efficiency in potential biomedical applications.

Acknowledgments

JAC is a Concordia University Research Chair in Nanoscience and is grateful to Concordia University for financial support for his research. He is also grateful for financial support from the Natural Sciences and Engineering Research Council (NSERC). AMI acknowledges financial support from Concordia University under the Frederick Lowy Scholars Fellowship. DCRB acknowledges financial support from Colciencias under the Convocatoria Exterior 2012-568 Program.

Disclosure statement

No potential conflict of interest was reported by the authors.

Funding

This work was supported by the Natural Sciences and Engineering Research Council of Canada [grant number 1950-2011].

References

- [1] R.P. Feynman, *Eng. Sci.* 23 (1960) p.22–36.
- [2] G.L. Prasad, *Biomedical applications of nanoparticles*, in *Safety of Nanoparticles*, T.J. Webster, eds., Springer, New York, 2009, p. 89–109.
- [3] J. Key and J.F. Leary, *Int. J. Nanomed.* 9 (2014) p.711–726.
- [4] J.C. De La Vega and U.O. Häfeli, *Contrast Media Mol. Imaging* 10 (2015) p.81–95.
- [5] J. Shen, L. Zhao and G. Han, *Adv. Drug Delivery Rev.* 65 (2013) p.744–755.
- [6] C.E. Probst, P. Zrazhevskiy, V. Bagalkot and X. Gao, *Adv. Drug Delivery Rev.* 65 (2013) p.703–718.
- [7] R. Vinhas, M. Cordeiro, F.F. Carlos, S. Mendo, A.R. Fernandes, S. Figueiredo and P.V. Baptista, *J. Nanobiosensors Dis. Diagn.* 4 (2015) p. 11–23.
- [8] A. Mooradian, *Phys. Rev. Lett.* 22 (1969) p.185–187.

- [9] H. Liao, C.L. Nehl and J.H. Hafner, *Nanomedicine* 1 (2006) p.201–208.
- [10] G. Mie, *Annalen der Physik [Annals of Physics]* (in German) 330 (1908) p.377–445.
- [11] P.K. Jain, K.S. Lee, I.H. El-Sayed and M.A. El-Sayed, *Shape Compos: Appl. Biol. Imaging Biomed. J. Phys. Chem. B* 110 (2006) p.7238–7248.
- [12] J. Turkevich, P.C. Stevenson and J. Hillier, *Discuss. Faraday Soc.* 11 (1951) p.55–75.
- [13] M. Brust, M. Walker, D. Bethell, D.J. Schiffrin and R. Whyman, *J. Chem. Soc. Chem. Commun.* 7 (1994) p.801–802.
- [14] X. Huang and M.A. El-Sayed, *J. Adv. Res.* 1 (2010) p.13–28.
- [15] S.J. Oldenburg, R.D. Averitt, S.L. Westcott and N.J. Halas, *Chem. Phys. Lett.* 288 (1998) p.243–247.
- [16] Y. Sun, B.T. Mayers and Y. Xia, *Nano Lett.* 2 (2002) p.481–485.
- [17] B. Nikoobakht and M.A. El-Sayed, *Chem. Mater.* 15 (2003) p.1957–1962.
- [18] R. Gui, H. Jin, Z. Wang and L. Tan, *Coord. Chem. Rev.* 296 (2015) p.91–124.
- [19] P.M. Allen and M.G. Bawendi, *J. Am. Chem. Soc.* 130 (2008) p.9240–9241.
- [20] W.R. Algar, K. Susumu, J.B. Delehanty and I.L. Medintz, *Anal. Chem.* 83 (2011) p.8826–8837.
- [21] K.D. Wegner and N. Hildebrandt, *Chem. Soc. Rev.* 44 (2015) p.4792–4834.
- [22] P. Alivisatos, *Nat. Biotechnol.* 22 (2004) p.47–52.
- [23] A.P. Alivisatos, W. Gu and C. Larabell, *Annu. Rev. Biomed. Eng.* 7 (2005) p.55–76.
- [24] O. Chen, J. Zhao, V.P. Chauhan, J. Cui, C. Wong, D.K. Harris, H. Wei, H.-S. Han, D. Fukumura, R.K. Jain and M.G. Bawendi, *Nat. Mater.* 12 (2013) p.445–451.
- [25] C. Dong, H. Liu, A. Zhang and J. Ren, *Chem. Eur. J.* 20 (2014) p.1940–1946.
- [26] C.B. Murray, D.J. Norris and M.G. Bawendi, *J. Am. Chem. Soc.* 115 (1993) p.8706–8715.
- [27] Z.A. Peng and X. Peng, *J. Am. Chem. Soc.* 123 (2001) p.183–184.
- [28] C.M. Evans, L.C. Cass, K.E. Knowles, D.B. Tice, R.P.H. Chang and E.A. Weiss, *J. Coord. Chem.* 65 (2012) p.2391–2414.
- [29] W. Chen, W. Cao, J. Hao and K. Wang, *Mater. Lett.* 139 (2015) p.98–100.
- [30] X. Peng, L. Manna, W. Yang, J. Wickham, E. Scher, A. Kadavanich and A.P. Alivisatos, *Nature* 404 (2000) p.59–61.
- [31] W.-C. Law, K.-T. Yong, I. Roy, H. Ding, R. Hu, W. Zhao and P.N. Prasad, *Small* 5 (2009) p.1302–1310.
- [32] H. Zhang, L. Wang, H. Xiong, L. Hu, B. Yang and W. Li, *Adv. Mater.* 15 (2003) p.1712–1715.
- [33] Y. He, L.-M. Sai, H.-T. Lu, M. Hu, W.-Y. Lai, Q.-L. Fan, L.-H. Wang and W. Huang, *Chem. of Mater.* 19 (2007) p.359–365.
- [34] G. Blasse and B.C. Grabmaier, *Luminescent Materials*, Springer, Berlin, 1994.
- [35] F. Wang and X. Liu, *J. Am. Chem. Soc.* 130 (2008) p.5642–5643.
- [36] K. Konig, *J. Microsc.* 200 (2000) p.83–104.
- [37] D.C. Rodriguez Burbano, R. Naccache and J.A. Capobianco, *Chapter 273 – Near-IR triggered photon upconversion: imaging, detection, and therapy*, in *Handbook on the Physics and Chemistry of Rare Earths*, B. Jean-Claude and K.P. Vitalij, eds., Amsterdam: Elsevier, 2015, p. 273–347.
- [38] R. Naccache, Q. Yu and J.A. Capobianco, *Adv. Opt. Mater.* 3 (2015) p.482–509.
- [39] C. Renero-Lecuna, R. Martín-Rodríguez, R. Valiente, J. González, F. Rodríguez, K.W. Krämer and H.U. Güdel, *Chem. Mater.* 23 (2011) p.3442–3448.
- [40] F. Wang and X. Liu, *Chem. Soc. Rev.* 38 (2009) p.976–989.
- [41] J.-C. Boyer, L.A. Cuccia and J.A. Capobianco, *Nano Lett.* 7 (2007) p.847–852.
- [42] F. Vetrone, R. Naccache, V. Mahalingam, C.G. Morgan and J.A. Capobianco, *Adv. Funct. Mater.* 19 (2009) p.2924–2929.
- [43] F. Wang and X. Liu, *J. Am. Chem. Soc.* 130 (2008) p.5642–5643.

- [44] S. Heer, K. Kömpe, H.U. Güdel and M. Haase, *Adv. Mater.* 16 (2004) p.2102–2105.
- [45] S. Yajuan, C. Yue, T. Lijin, Y. Yi, K. Xianggui, Z. Junwei and Z. Hong, *Nanotechnology* 18 (2007) p.275609.
- [46] H.-X. Mai, Y.-W. Zhang, L.-D. Sun and C.-H. Yan, *J. Phys. Chem. C* 111 (2007) p.13730–13739.
- [47] C. Li, J. Yang, Z. Quan, P. Yang, D. Kong and J. Lin, *Chem. Mater.* 19 (2007) p.4933–4942.
- [48] K. Van den Eeckhout, P.F. Smet and D. Poelman, *Materials* 3 (2010) p.2536.
- [49] Y. Zhuang, Y. Katayama, J. Ueda and S. Tanabe, *Opt. Mater.* 36 (2014) p.1907–1912.
- [50] A. Bessière, S.K. Sharma, N. Basavaraju, K.R. Priolkar, L. Binet, B. Viana, A.J.J. Bos, T. Maldiney, C. Richard, D. Scherman and D. Gourier, *Chem. Mater.* 26 (2014) p.1365–1373.
- [51] D.C. Rodríguez Burbano, E.M. Rodríguez, P. Dorenbos, M. Bettinelli and J.A. Capobianco, *J. Mater. Chem. C* 2 (2014) p. 228–231.
- [52] S.K. Singh, *RSC Adv.* 4 (2014) p.58674–58698.
- [53] D.C. Rodríguez Burbano, S.K. Sharma, P. Dorenbos, B. Viana and J.A. Capobianco, *Adv. Opt. Mater.* 3 (2015) p.551–557.
- [54] X. Sun, X. Huang, J. Guo, W. Zhu, Y. Ding, G. Niu, A. Wang, D.O. Kiesewetter, Z.L. Wang, S. Sun and X. Chen, *J. Am. Chem. Soc.* 136 (2014) p.1706–1709.
- [55] A.M. Smith, M.C. Mancini and S. Nie, *Nat. Nanotechnol.* 4 (2009) p.710–711.
- [56] S.C. Ray, A. Saha, N.R. Jana and R. Sarkar, *J. Phys. Chem. C* 113 (2009) p.18546–18551.
- [57] A. Zhao, Z. Chen, C. Zhao, N. Gao, J. Ren and X. Qu, *Carbon* 85 (2015) p.309–327.
- [58] P.G. Luo, S. Sahu, S.-T. Yang, S.K. Sonkar, J. Wang, H. Wang, G.E. LeCroy, L. Cao and Y.-P. Sun, *J. Mater. Chem. B* 1 (2013) p.2116–2127.
- [59] S.N. Baker and G.A. Baker, *Angew. Chem. Int. Ed.* 49 (2010) p.6726–6744.
- [60] Y.-P. Sun, B. Zhou, Y. Lin, W. Wang, K.A.S. Fernando, P. Pathak, M.J. Meziani, B.A. Harruff, X. Wang, H. Wang, P.G. Luo, H. Yang, M.E. Kose, B. Chen, L.M. Veca and S.-Y. Xie, *J. Am. Chem. Soc.* 128 (2006) p.7756–7757.
- [61] L. Cao, M.J. Meziani, S. Sahu and Y.-P. Sun, *Acc. Chem. Res.* 46 (2013) p.171–180.
- [62] H. Li, Z. Kang, Y. Liu and S.-T. Lee, *J. Mater. Chem.* 22 (2012) p.24230–24253.
- [63] Q.-L. Zhao, Z.-L. Zhang, B.-H. Huang, J. Peng, M. Zhang and D.-W. Pang, *Chem. Commun.* 41 (2008) p.5116–5118.
- [64] Z.-A. Qiao, Y. Wang, Y. Gao, H. Li, T. Dai, Y. Liu and Q. Huo, *Chem. Commun.* 46 (2010) p.8812–8814.
- [65] X. Xu, R. Ray, Y. Gu, H.J. Ploehn, L. Gearheart, K. Raker and W.A. Scrivens, *J. Am. Chem. Soc.* 126 (2004) p.12736–12737.
- [66] J. Zhou, C. Booker, R. Li, X. Zhou, T.-K. Sham, X. Sun and Z. Ding, *J. Am. Chem. Soc.* 129 (2007) p.744–745.
- [67] H. Liu, T. Ye and C. Mao, *Angew. Chem. Int. Ed.* 46 (2007) p.6473–6475.
- [68] S.-L. Hu, K.-Y. Niu, J. Sun, J. Yang, N.-Q. Zhao and X.-W. Du, *J. Mater. Chem.* 19 (2009) p.484–488.
- [69] R. Liu, D. Wu, S. Liu, K. Koynov, W. Knoll and Q. Li, *Angew. Chem. Int. Ed.* 48 (2009) p.4598–4601.
- [70] C.-W. Lai, Y.-H. Hsiao, Y.-K. Peng and P.-T. Chou, *J. Mater. Chem.* 22 (2012) p.14403–14409.
- [71] H. Zhu, X. Wang, Y. Li, Z. Wang, F. Yang and X. Yang, *Chem. Commun.* (2009) p.5118–5120.
- [72] X. Jia, J. Li and E. Wang, *Nanoscale* 4 (2012) p.5572–5575.
- [73] G. Sahay, D.Y. Alakhova and A.V. Kabanov, *J. Controlled Release* 145 (2010) p.182–195.
- [74] J. Wang, J.D. Byrne, M.E. Napier and J.M. DeSimone, *Small* 7 (2011) p.1919–1931.

- [75] Y. Geng, P. Dalhaimer, S. Cai, R. Tsai, M. Tewari, T. Minko and D.E. Discher, *Nanotechnol.* 2 (2007) p.249–255.
- [76] A. Verma and F. Stellacci, *Small* 6 (2010) p.12–21.
- [77] F.J. Arriagada and K. Osseo-Asare, *J. Colloid Interface Sci.* 211 (1999) p.210–220.
- [78] W. Stöber, A. Fink and E. Bohn, *J. Colloid Interface Sci.* 26 (1968) p.62–69.
- [79] J. Cichos and M. Karbowski, *J. Mater. Chem. B* 2 (2014) p.556–568.
- [80] J.V. Jokerst, T. Lobovkina, R.N. Zare and S.S. Gambhir, *Nanomedicine* 6 (2011) p. 715–728.
- [81] L. van Vlerken, T. Vyas and M. Amiji, *Pharm. Res.* 24 (2007) p.1405–1414.
- [82] J. Weingart, P. Vabbilisetty and X.-L. Sun, *Adv. Colloid Interface Sci.* 197–198 (2013) p.68–84.
- [83] I. Brigger, C. Dubernet and P. Couvreur, *Adv. Drug Delivery Rev.* 54 (2002) p.631–651.
- [84] J. Sudimack and R.J. Lee, *Adv. Drug Delivery Rev.* 41 (2000) p.147–162.
- [85] P. Ponka and C.N. Lok, *Int. J. Biochem. Cell Biol.* 31 (1999) p.1111–1137.
- [86] F.X. Gu, R. Karnik, A.Z. Wang, F. Alexis, E. Levy-Nissenbaum, S. Hong, R.S. Langer and O.C. Farokhzad, *Nano Today* 2 (2007) p.14–21.
- [87] M.v. Mehren, G.P. Adams and L.M. Weiner, *Annu. Rev. Med.* 54 (2003) p. 343–369.
- [88] R. Brissette, J.K. Prendergast and N.I. Goldstein, *Curr. Opin. Drug Discovery Dev.* 9 (2006) p.363–369.
- [89] V. Biju, *Chem. Soc. Rev* 43 (2014) p.744–764.
- [90] R. Weissleder and V. Ntziachristos, *Nat. Med.* 9 (2003) p.123–128.
- [91] T.G. Phan and A. Bullen, *Immunol. Cell Biol.* 88 (2010) p.438–444.
- [92] J. Meek, *Dev. Sci.* 5 (2002) p.371–380.
- [93] M. Bruchez, M. Moronne, P. Gin, S. Weiss and A.P. Alivisatos, *Science* 281 (1998) p.2013–2016.
- [94] B.A. Kairdolf, A.M. Smith, T.H. Stokes, M.D. Wang, A.N. Young and S. Nie, *Annu. Rev. Anal. Chem.* 6 (2013) p.143–162.
- [95] J. Li and J.-J. Zhu, *The Analyst* 138 (2013) p.2506–2515.
- [96] O. Mashinchian, M. Johari-Ahar, B. Ghaemi, M. Rashidi, J. Barar and Y. Omid, *Bioimpacts* 4 (2014) p.149–166.
- [97] Y. Chen, Y. Zhang, W. Liang and X. Li, *Nanomed. Nanotechnol. Biol. Med.* 8 (2012) p.1267–1270.
- [98] N. Verellen, D. Denkova, B.D. Clercq, A.V. Silhanek, M. Ameloot, P.V. Dorpe and V.V. Moshchalkov, *ACS Photonics* 2 (2015) p.410–416.
- [99] X. Jin, H. Li, S. Wang, N. Kong, H. Xu, Q. Fu, H. Gu and J. Ye, *Nanoscale* 6 (2014) p.14360–14370.
- [100] Y. Hsiangkuo, G.K. Christopher, H. Hanjun, M.W. Christy, A.G. Gerald and V.-D. Tuan, *Nanotechnology* 23 (2012) p.075102.
- [101] L. Tong, C.M. Cobley, J. Chen, Y. Xia and J.-X. Cheng, *Angew. Chem. Int. Ed.* 49 (2010) p.3485–3488.
- [102] D.K. Chatterjee, A.J. Rufaihah and Y. Zhang, *Biomaterials* 29 (2008) p.937–943.
- [103] N. Bogdan, E.M. Rodríguez, F. Sanz-Rodríguez, M.C. Iglesias de la Cruz, A. Juarranz, D. Jaque, J.G. Solé and J.A. Capobianco, *Nanoscale* 4 (2012) p. 3647–3650.
- [104] X. Wu, G. Chen, J. Shen, Z. Li, Y. Zhang and G. Han, *Bioconjugate Chem.* 26 (2015) p.166–175.
- [105] M.V. DaCosta, S. Doughan, Y. Han and U.J. Krull, *Analy. Chim. Acta* 832 (2014) p.1–33.
- [106] Y. Yang, *Microchim. Acta* 181 (2014) p.263–294.
- [107] B. Kasibabu, *J. Fluoresc.* 25 (2015) p.803–810.
- [108] Y. Song, W. Shi, W. Chen, X. Li and H. Ma, *J. Mater. Chem.* 22 (2012) p.12568–12573.

- [109] X. Zhang, S. Wang, C. Zhu, M. Liu, Y. Ji, L. Feng, L. Tao and Y. Wei, *J. Colloid Interface Sci.* 397 (2013) p.39–44.
- [110] J.-H. Liu, L. Cao, G.E. LeCroy, P. Wang, M.J. Mezziani, Y. Dong, Y. Liu, P.G. Luo and Y.-P. Sun, *ACS Appl. Mater. Interfaces* 7 (2015) p.19439–19445.
- [111] T. Maldiney, M.U. Kaikkonen, J. Seguin, Q. le Masne de Chermont, M. Bessodes, K.J. Airene, S. Ylä-Herttuala, D. Scherman and C. Richard, *Bioconjugate Chem.* 23 (2012) p.472–478.
- [112] T. Maldiney, A. Bessière, J. Seguin, E. Teston, S.K. Sharma, B. Viana, A.J.J. Bos, P. Dorenbos, M. Bessodes, D. Gourier, D. Scherman and C. Richard, *Nat. Mater.* 13 (2014) p.418–426.
- [113] L. Zhang, J. Lei, J. Liu, F. Ma and H. Ju, *Biomaterials* 67 (2015) p.323–334.
- [114] T. Maldiney, G. Byk, N. Wattier, J. Seguin, R. Khandadash, M. Bessodes, C. Richard and D. Scherman, *Int. J. Pharm.* 423 (2012) p.102–107.
- [115] L. Smith, Z. Kuncic, K. Ostrikov and S. Kumar, *J. Nanomater.* 2012 (2012) p.7.
- [116] M.N. Rhyner, A.M. Smith, X. Gao, H. Mao, L. Yang and S. Nie, *Nanomedicine 1* (2006) p.209–217.
- [117] X. Gao, Y. Cui, R.M. Levenson, L.W.K. Chung and S. Nie, *Nat. Biotechnol.* 22 (2004) p.969–976.
- [118] J. Gao, K. Chen, R. Luong, D.M. Bouley, H. Mao, T. Qiao, S.S. Gambhir and Z. Cheng, *Nano Lett.* 12 (2012) p.281–286.
- [119] C. Li, Y. Zhang, M. Wang, Y. Zhang, G. Chen, L. Li, D. Wu and Q. Wang, *Biomaterials* 35 (2014) p.393–400.
- [120] L.-W. Wang, C.-W. Peng, C. Chen and Y. Li, *Breast Cancer Res. Treat.* 151 (2015) p.7–17.
- [121] M.-X. Zhao and E.-Z. Zeng, *Nanoscale Res. Lett.* 10 (2015) p.171.
- [122] L. Cheng, K. Yang, S. Zhang, M. Shao, S. Lee and Z. Liu, *Nano Res.* 3 (2010) p.722–732.
- [123] Y.-F. Wang, G.-Y. Liu, L.-D. Sun, J.-W. Xiao, J.-C. Zhou and C.-H. Yan, *ACS Nano* 7 (2013) p.7200–7206.
- [124] Y. Yu, T. Huang, Y. Wu, X. Ma, G. Yu and J. Qi, *Pathol. Oncol. Res.* 20 (2014) p.335–341.
- [125] Q. le Masne de Chermont, C. Chaneac, J. Seguin, F. Pelle, S. Maitrejean, J.-P. Jolivet, D. Gourier, M. Bessodes and D. Scherman, *Proc. Nat. Acad. Sci.* 104 (2007) p.9266–9271.
- [126] J. Cheon and J.-H. Lee, *Acc. Chem. Res.* 41 (2008) p.1630–1640.
- [127] L. Zeng, L. Xiang, W. Ren, J. Zheng, T. Li, B. Chen, J. Zhang, C. Mao, A. Li and A. Wu, *RSC Adv.* 3 (2013) p.13915–13925.
- [128] G.J. Stasiuk, S. Tamang, D. Imbert, C. Gateau, P. Reiss, P. Fries and M. Mazzanti, *Dalton Trans.* 42 (2013) p.8197–8200.
- [129] A. Abdukayum, C.-X. Yang, Q. Zhao, J.-T. Chen, L.-X. Dong and X.-P. Yan, *Anal. Chem.* 86 (2014) p.4096–4101.
- [130] T. Jahanbin, M. Gaceur, H. Gros-Dagnac, S. Benderbous and S. Merah, *J. Nanopart. Res.* 17 (2015) p.1–12.
- [131] R. Naccache, P. Chevallier, J. Lagueux, Y. Gossuin, S. Laurent, L. Vander Elst, C. Chilian, J.A. Capobianco and M.-A. Fortin, *Adv. Healthcare Mater.* 2 (2013) p.1478–1488.
- [132] F. Hu, C. Li, Y. Zhang, M. Wang, D. Wu and Q. Wang, *Nano Res.* 8 (2015) p.1637–1647.
- [133] S. Carron, Q.Y. Li, L. Vander Elst, R.N. Muller, T.N. Parac-Vogt and J.A. Capobianco, *Dalton Trans.* 44 (2015) p.11331–11339.
- [134] Y. Sun, M. Yu, S. Liang, Y. Zhang, C. Li, T. Mou, W. Yang, X. Zhang, B. Li, C. Huang and F. Li, *Biomaterials* 32 (2011) p.2999–3007.
- [135] Q. Liu, M. Chen, Y. Sun, G. Chen, T. Yang, Y. Gao, X. Zhang and F. Li, *Biomaterials* 32 (2011) p.8243–8253.
- [136] Y. Sun, X. Zhu, J. Peng and F. Li, *ACS Nano* 7 (2013) p.11290–11300.

- [137] M. Patt, A. Schildan, B. Habermann, O. Mishchenko, J.T. Patt and O. Sabri, *J. Radioanal. Nucl. Chem.* 283 (2010) p.487–491.
- [138] W. Guo, X. Sun, O. Jacobson, X. Yan, K. Min, A. Srivatsan, G. Niu, D.O. Kiesewetter, J. Chang and X. Chen, *ACS Nano* 9 (2015) p.488–495.
- [139] H. Hu, P. Huang, O.J. Weiss, X. Yan, X. Yue, M.G. Zhang, Y. Tang, L. Nie, Y. Ma, G. Niu, K. Wu and X. Chen, *Biomaterials* 35 (2014) p.9868–9876.
- [140] W. Cai and H. Hong, *Am. J. Nucl. Med. Mol. Imaging* 2 (2012) p.136–140.
- [141] C. Zhang, Z. Zhou, Q. Qian, G. Gao, C. Li, L. Feng, Q. Wang and D. Cui, *J. Mater. Chem. B* 1 (2013) p.5045–5053.
- [142] J.-T. Song, X.-Q. Yang, X.-S. Zhang, D.-M. Yan, M.-H. Yao, M.-Y. Qin and Y.-D. Zhao, *Dalton Trans.* 44 (2015) p.11314–11320.
- [143] X. Zhai, P. Lei, P. Zhang, Z. Wang, S. Song, X. Xu, X. Liu, J. Feng and H. Zhang, *Biomaterials* 65 (2015) p.115–123.
- [144] J. Ding, Y. Wang, M. Ma, Y. Zhang, S. Lu, Y. Jiang, C. Qi, S. Luo, G. Dong, S. Wen, Y. An and N. Gu, *Biomaterials* 34 (2013) p.209–216.
- [145] D.-H. Hu, Z.-H. Sheng, P.-F. Zhang, D.-Z. Yang, S.-H. Liu, P. Gong, D.-Y. Gao, S.-T. Fang, Y.-F. Ma and L.-T. Cai, *Nanoscale* 5 (2013) p.1624–1628.
- [146] J. Zhou, X. Zhu, M. Chen, Y. Sun and F. Li, *Biomaterials* 33 (2012) p.6201–6210.
- [147] F. Liu, X. He, L. Liu, H. You, H. Zhang and Z. Wang, *Biomaterials* 34 (2013) p.5218–5225.
- [148] H. Xing, W. Bu, S. Zhang, X. Zheng, M. Li, F. Chen, Q. He, L. Zhou, W. Peng, Y. Hua and J. Shi, *Biomaterials* 33 (2012) p.1079–1089.
- [149] X. Zhu, J. Zhou, M. Chen, M. Shi, W. Feng and F. Li, *Biomaterials* 33 (2012) p.4618–4627.
- [150] Q. Xiao, W. Bu, Q. Ren, S. Zhang, H. Xing, F. Chen, M. Li, X. Zheng, Y. Hua, L. Zhou, W. Peng, H. Qu, Z. Wang, K. Zhao and J. Shi, *Biomaterials* 33 (2012) p.7530–7539.
- [151] J. Lee, T.S. Lee, J. Ryu, S. Hong, M. Kang, K. Im, J.H. Kang, S.M. Lim, S. Park and R. Song, *J. Nucl. Med.* 54 (2013) p.96–103.
- [152] J. Zhou, M. Yu, Y. Sun, X. Zhang, X. Zhu, Z. Wu, D. Wu and F. Li, *Biomaterials* 32 (2011) p.1148–1156.
- [153] J. Rieffel, F. Chen, J. Kim, G. Chen, W. Shao, S. Shao, U. Chitgupi, R. Hernandez, S.A. Graves, R.J. Nickles, P.N. Prasad, C. Kim, W. Cai and J.F. Lovell, *Adv. Mater.* 27 (2015) p.1785–1790.
- [154] E. Pérez-Herrero and A. Fernández-Medarde, *Eur. J. Pharm. Biopharm.* 93 (2015) p.52–79.
- [155] W. Chih-Jen, T.S. Calvin, A.A. Ibrahim, H. Yu-Jie and F. Jia-You, *Nanotechnology* 24 (2013) p.325101.
- [156] K.C. Weng, R. Hashizume, C.O. Noble, L.P. Serwer, D.C. Drummond, D.B. Kirpotin, A.M. Kuwabara, L.X. Chao, F.F. Chen, C.D. James and J.W. Park, *Nanomedicine* 8 (2013) p.1913–1925.
- [157] W. Wang, D. Cheng, F. Gong, X. Miao and X. Shuai, *Adv. Mater.* 24 (2012) p.115–120.
- [158] P. Zhang, F. Cheng, R. Zhou, J. Cao, J. Li, C. Burda, Q. Min and J.-J. Zhu, *Angew. Chem. Int. Ed.* 53 (2014) p.2371–2375.
- [159] Y. Wang, S. Song, J. Liu, D. Liu and H. Zhang, *Angew. Chem. Int. Ed.* 54 (2015) p.536–540.
- [160] R. Gui, Y. Wang and J. Sun, *Colloids Surf. B* 116 (2014) p.518–525.
- [161] J. Shi, X. Sun, J. Li, H. Man, J. Shen, Y. Yu and H. Zhang, *Biomaterials* 37 (2015) p.260–270.
- [162] S.S. Lucky, K.C. Soo and Y. Zhang, *Chem. Rev.* 115 (2015) p.1990–2042.
- [163] J. Zhao, W. Wu, J. Sun and S. Guo, *Chem. Soc. Rev.* 42 (2013) p.5323–5351.
- [164] C. Zhang, C. Li, Y. Liu, J. Zhang, C. Bao, S. Liang, Q. Wang, Y. Yang, H. Fu, K. Wang and D. Cui, *Adv. Funct. Mater.* 25 (2015) p.1314–1325.

- [165] N.-T.Chen, K.-C. Tang, M.F. Chung, S.H. Cheng, C.M. Huang, C.H. Chu, P.T. Chou, J.S. Souris, C.T. Chen, C.Y. Mou and L.W. Lo, *Theranostics* 4 (2014) pp.798–807.
- [166] J. Wang, Z. Zhang, S. Zha, Y. Zhu, P. Wu, B. Ehrenberg and J.-Y. Chen, *Biomaterials* 35 (2014) p.9372–9381.
- [167] I.V. Martynenko, V.A. Kuznetsova, A.O. Orlova, P.A. Kanaev, V.G. Maslov, A. Loudon, V. Zaharov and P. Parfenov, *Nanotechnology* 26 (2015) p.055102–55105.
- [168] Q. Yu, E.M. Rodriguez, R. Naccache, P. Forgione, G. Lamoureux, F. Sanz-Rodriguez, D. Scheglmann and J.A. Capobianco, *Chem. Commun.* 50 (2014) p.12150–12153.
- [169] B. Hou, B. Zheng, X. Gong, H. Wang, S. Wang, Z. Liao, X. Li, X. Zhang and J. Chang, *J. Mater. Chem. B* 3 (2015) p.3531–3540.
- [170] H. Li, S. Song, W. Wang and K. Chen, *Dalton Trans.* 44 (2015) p.16081–16090.
- [171] X. Wang, K. Liu, G. Yang, L. Cheng, L. He, Y. Liu, Y. Li, L. Guo and Z. Liu, *Nanoscale* 6 (2014) p.9198–9205.
- [172] R. Lv, C. Zhong, R. Li, P. Yang, F. He, S. Gai, Z. Hou, G. Yang and J. Lin, *Chem. Mater.* 27 (2015) p.1751–1763.
- [173] Z. Hou, Y. Zhang, K. Deng, Y. Chen, X. Li, X. Deng, Z. Cheng, H. Lian, C. Li and J. Lin, *ACS Nano* 9 (2015) p.2584–2599.
- [174] L.E. Zhang, L. Zeng, Y. Pan, S. Luo, W. Ren, A. Gong, X. Ma, H. Liang, G. Lu and A. Wu, *Biomaterials* 44 (2015) p.82–90.
- [175] S.S. Lucky, N. Muhammad Idris, Z. Li, K. Huang, K.C. Soo and Y. Zhang, *ACS Nano* 9 (2015) p.191–205.
- [176] M. Yin, E. Ju, Z. Chen, Z. Li, J. Ren and X. Qu, *Chem. A Eur. J.* 20 (2014) p.14012–14017.
- [177] L.C. Chao Wang and Z. Liu, *Theranostics* 3 (2013) pp.317–330.
- [178] V. Srivastava, D. Gusain and Y.C. Sharma, *Ind. Eng. Chem. Res.* 54 (2015) p.6209–6233.
- [179] A. Gnach, T. Lipinski, A. Bednarkiewicz, J. Rybka and J.A. Capobianco, *Chem. Soc. Rev.* 44 (2015) p.1561–1584.
- [180] S.-J. Choi, J. Lee, J. Jeong and J.-H. Choy, *Mol. Cell. Toxicol.* 9 (2013) p.205–210.
- [181] N. Lewinski, V. Colvin and R. Drezek, *Small* 4 (2008) p.26–49.
- [182] S.A. Love, M.A. Maurer-Jones, J.W. Thompson, Y.-S. Lin and C.L. Haynes, *Annu. Rev. Anal. Chem.* 5 (2012) p.181–205.
- [183] J. Ai, E. Biazar, M. Jafarpour, M. Montazeri, A. Majdi, S. Aminifard, M. Zafari, H.R. Akbari and H.G. Rad, *Int. J. Nanomed.* 6 (2011) p.1117–1127.
- [184] A. Elsaesser and C.V. Howard, *Adv. Drug Delivery Rev.* 64 (2012) p.129–137.
- [185] S.J. Soenen, P. Rivera-Gil, J.-M. Montenegro, W.J. Parak, S.C. De Smedt and K. Braeckmans, *Nano Today* 6 (2011) p.446–465.
- [186] F. Wu, S. Bhansali, W. Law, E. Bergey, P. Prasad and M. Morris, *Pharm. Res.* 29 (2012) p.1843–1853.
- [187] D.E. Owens III and N.A. Peppas, *Int. J. Pharm.* 307 (2006) p.93–102.
- [188] M. Longmire, P.L. Choyke and H. Kobayashi, *Nanomedicine* 3 (2008) pp.703–717.
- [189] M. Lundqvist, J. Stigler, G. Elia, I. Lynch, T. Cedervall and K.A. Dawson, *Proc. Nat. Acad. Sci.* 105 (2008) p.14265–14270.
- [190] D.B. Warheit, *Mater. Today* 7 (2004) p.32–35.
- [191] B. Fubini and A. Hubbard, *Free Rad. Biol. Med.* 34 (2003) p.1507–1516.
- [192] J. Chen, J.A. Hessler, K. Putchakayala, B.K. Panama, D.P. Khan, S. Hong, D.G. Mullen, S.C. DiMaggio, A. Som, G.N. Tew, A.N. Lopatin, J.R. Baker, M.M.B. Holl and B.G. Orr, *J. Phys. Chem. B* 113 (2009) p.11179–11185.
- [193] H.J. Johnston, G. Hutchison, F.M. Christensen, S. Peters, S. Hankin and V. Stone, *Crit. Rev. Toxicol.* 40 (2010) p.328–346.
- [194] N. Khlebtsov and L. Dykman, *Chem. Soc. Rev.* 40 (2011) p.1647–1671.

- [195] A.M. El Badawy, R.G. Silva, B. Morris, K.G. Scheckel, M.T. Suidan and T.M. Tolaymat, *Environ. Sci. Technol.* 45 (2011) p.283–287.
- [196] R. de Lima, A.B. Seabra and N. Durán, *J. Appl. Toxicol.* 32 (2012) p.867–879.
- [197] A. Valizadeh, H. Mikaeili, M. Samiei, S. Farkhani, N. Zarghami, M. Kouhi, A. Akbarzadeh and S. Davaran, *Nanoscale Res. Lett.* 7 (2012) p.1–14.
- [198] K.-T. Yong, W.-C. Law, R. Hu, L. Ye, L. Liu, M.T. Swihart and P.N. Prasad, *Chem. Soc. Rev.* 42 (2013) p.1236–1250.
- [199] Y. Wang, R. Hu, G. Lin, I. Roy and K.-T. Yong, *ACS Appl. Mater. Interfaces* 5 (2013) p.2786–2799.
- [200] C.E. Bradburne, J.B. Delehanty, K. Boeneman Gemmill, B.C. Mei, H. Mattoussi, K. Susumu, J.B. Blanco-Canosa, P.E. Dawson and I.L. Medintz, *Bioconjugate Chem.* 24 (2013) p.1570–1583.
- [201] T. Wu and M. Tang, *Inhal. Toxicol.* 26 (2014) p.128–139.
- [202] K. Wang, J. Ma, M. He, G. Gao, H. Xu, J. Sang, Y. Wang, B. Zhao and D. Cui, *Theranostics* 3 (2013) p.258–266.
- [203] M.V. DaCosta, S. Doughan, Y. Han and U.J. Krull, *Anal. Chim. Acta* 832 (2014) p.1–33.
- [204] G. Chen and G. Han, *Theranostics* 3 (2013) p.289–291.
- [205] J.-H. Liu, S.-T. Yang, X.-X. Chen and H. Wang, *Curr. Drug Metab.* 13 (2012) p.1046–1056.